

Towards Solving the Gilbert-Pollak Conjecture via Large Language Models

Yisi Ke ^{*1} Tianyu Huang ^{*1} Yankai Shu ^{*1} Di He ¹ Jingchu Gai^{†2} Liwei Wang^{†1}

Abstract

The Gilbert-Pollak Conjecture (Gilbert & Pollak, 1968), also known as the Steiner Ratio Conjecture, states that for any finite point set in the Euclidean plane, the Steiner minimum tree has length at least $\sqrt{3}/2 \approx 0.866$ times that of the Euclidean minimum spanning tree (the Steiner ratio). A sequence of improvements through the 1980s culminated in a lower bound of 0.824, with no substantial progress reported over the past three decades. Recent advances in LLMs have demonstrated strong performance on contest-level mathematical problems, yet their potential for addressing open, research-level questions remains largely unexplored. In this work, we present a novel AI system for obtaining tighter lower bounds on the Steiner ratio. Rather than directly prompting LLMs to solve the conjecture, we task them with generating rule-constrained geometric lemmas implemented as executable code. These lemmas are then used to construct a collection of specialized functions, which we call verification functions, that yield theoretically certified lower bounds of the Steiner ratio. Through progressive lemma refinement driven by reflection, the system establishes a new certified lower bound of 0.8559 for the Steiner ratio. The entire research effort involves only thousands of LLM calls, demonstrating the strong potential of LLM-based systems for advanced mathematical research.

1. Introduction

The Gilbert-Pollak Conjecture (Gilbert & Pollak, 1968) stands as a seminal open problem in combinatorial optimization and computational geometry, with profound implications for geometric network design (Kahng & Robins, 1994) and operations research. Given a finite set of points

^{*}Equal contribution [†]Co-corresponding authors. ¹Peking University ²Carnegie Mellon University, Machine Learning Department. Correspondence to: Jingchu Gai <jgai@andrew.cmu.edu>, Liwei Wang <wanglw@pku.edu.cn>.

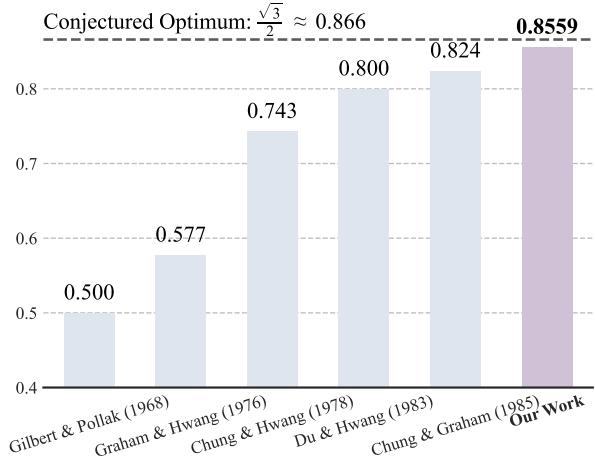


Figure 1. Progress on Steiner Ratio Lower Bound

in the Euclidean plane, the Steiner Minimal Tree (SMT) is the shortest network that connects all points, allowing the introduction of additional auxiliary nodes, known as Steiner points. The Steiner ratio is the infimum of the ratio between the length of the SMT and that of the Minimum Spanning Tree (MST). Gilbert & Pollak (1968) conjectured that this ratio is lower-bounded by $\sqrt{3}/2$. Subsequent work has sought to establish tight lower bounds approaching this conjectured optimum. Remarkably, no further improvements have been reported over nearly four decades, reflecting the difficulty of the problem. See Figure 1 and the Preliminaries for a summary of the relevant literature.

Recently, Large Language Models (LLMs) have demonstrated remarkable results in solving contest-level mathematics (Achim et al., 2025; Chervonyi et al., 2025). A natural next step is to explore whether these capabilities can be extended to tackling unsolved mathematical conjectures, such as the Gilbert-Pollak Conjecture. However, naïvely prompting LLMs to address such tasks often yields incorrect proofs with subtle logical gaps and fundamental misunderstandings of key concepts. Unlike canonical definitions commonly found in textbooks, research-level concepts appear only sparsely in training data. Compared to well-structured competition problems, open research problems exhibit a vastly larger and less constrained search space. As a result, models struggle to identify valid proof strategies and become substantially more prone to hallucination.

To address this challenge, we propose a novel AI system for automating theoretical discovery in the context of the

Gilbert–Pollak Conjecture. We first introduce a new mathematical tool, termed verification functions. We prove that identifying a valid collection of such functions yields a rigorous lower bound on the Steiner ratio, which serves as the system’s reward signal. To facilitate the search for valid collections of verification functions, we further decompose each verification function into two parametric lemmas, whose implementations are generated by LLMs as rule-constrained executable code. We also develop a reflection process that identifies key elements limiting further reward improvements and provides this information to the LLM, guiding subsequent generations to overcome the bottleneck. An overview of the system is illustrated in Figure 2.

Our proposed system has several key advantages over general LLM-based reasoning systems. By narrowing and concretizing the search space, the LLM can focus on generating simpler, more isolated, and more fundamental lemmas in executable code, making the overall objective significantly easier than attempting to solve the conjecture end to end. The verification function then integrates these lemmas into a rigorous computation of the lower bound, ultimately determining the final outcome. Moreover, rather than relying solely on a scalar reward signal, our reflection mechanism returns mathematically structured feedback to the LLM, enabling more effective and targeted iterative refinement.

Leveraging this AI system tailored to the Gilbert–Pollak Conjecture, we successfully improve the lower bound of the Steiner ratio from 0.824—the previous state-of-the-art result established by Chung & Graham (1985)—to 0.8559. Notably, the iterative refinement process requires only about ten iterations. The entire research effort involves only thousands of LLM calls, incurring a total cost of just a few hundred dollars, thereby demonstrating the strong potential of LLM-based systems for advanced mathematical research.

Reproducible codes and the final proof can be found in <https://github.com/keyisi2006/Steiner-Ratio>.

2. Related Works

The Gilbert-Pollak Conjecture. Originally proposed by Gilbert & Pollak (1968), this conjecture posits that the Steiner ratio is $\rho = \sqrt{3}/2$. Beyond its theoretical importance in combinatorial optimization, the conjecture holds significant implications for **Very Large Scale Integration (VLSI)** design and **network optimization** (Kahng & Robins, 1994; Du & Hu, 2008). While Gilbert and Pollak verified the conjecture for $n = 3$, subsequent work confirmed it for specific cases: $n = 4$ by Pollak (1978), $n = 5$ by Du et al. (1985), and $n = 6$ by Rubenstein & Thomas (1991). regarding the general lower bound for any n , significant efforts have pushed the value from an initial 0.5 to 0.57

(Graham & Hwang, 1976), 0.74 (Chung & Hwang, 1978), 0.8 (Du & Hwang, 1983), and finally to 0.824 (Chung & Graham, 1985). However, improving this bound further has remained an open challenge since 1985 due to the prohibitive complexity of the search space.

Solving Math Problems with LLMs. Recent advancements in LLMs have demonstrated remarkable potential in mathematical reasoning, extending from standard benchmarks to competition-level challenges. In specialized domains, Trinh et al. (2024) introduced AlphaGeometry, a neuro-symbolic system capable of solving IMO geometry problems without human demonstrations. To tackle broader formal reasoning, HyperTree Proof Search (Lample et al., 2022) pioneered the integration of Transformer-based policies with Monte-Carlo Tree Search (MCTS). Building on this direction, recent works leverage Reinforcement Learning (RL) within formal environments: AlphaProof (Google DeepMind, 2024) achieves silver-medal standards in Lean, while DeepSeek-Prover (Xin et al., 2024a;b) employs RL to establish state-of-the-art performance in open-ended theorem proving. To enhance reasoning reliability, InternLM-Math (Ying et al., 2024) leverages process supervision to verify intermediate steps. On the infrastructure front, Yang et al. (2023) developed LeanDojo, an open environment enabling large-scale training of these systems. Most recently, Goedel-Prover (Lin et al., 2025a;b) was introduced as a frontier model, achieving top performance among open-weight models on the MiniF2F benchmark.

AI for Scientific Discovery. Artificial Intelligence has catalyzed paradigm shifts across various scientific disciplines. In biology, AlphaFold (Jumper et al., 2021; 2020; Krokidis et al., 2025) revolutionized structural biology by predicting protein structures with atomic accuracy. In materials science, Merchant et al. (2023) leveraged graph neural networks to discover 2.2 million new crystals (GNoME), dramatically expanding the scale of stable materials known to humanity. Similarly, GraphCast (Lam et al., 2023) demonstrated that AI can model complex physical dynamics to outperform traditional weather forecasting. Moving towards algorithmic discovery, AlphaTensor (Fawzi et al., 2022) utilized reinforcement learning to discover matrix multiplication algorithms surpassing human-designed heuristics. More recently, the focus has shifted towards fully automated research frameworks; for instance, Lu et al. (2024); Yamada et al. (2025) proposed "The AI Scientist," where LLM-based agents independently generate ideas, execute experiments, and write manuscripts. Following this trajectory, we extend the exploratory capabilities of AI to the domain of Theoretical Mathematics, specifically targeting combinatorial optimization problems.

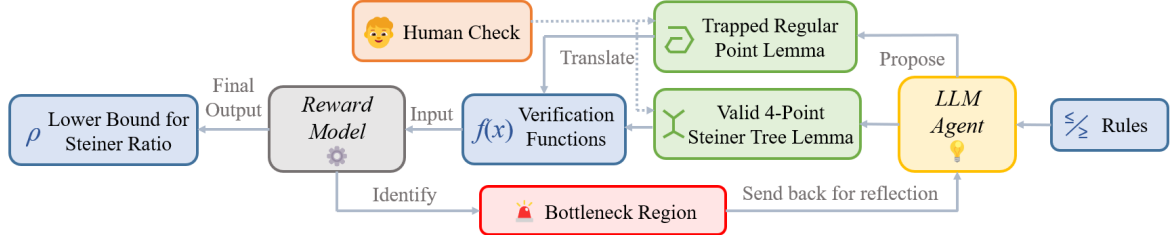


Figure 2. Illustration of our proposed LLM Math Research System for the Gilbert-Pollak Conjecture

3. Preliminary

Before presenting our method, we review the background of the Gilbert-Pollak Conjecture and introduce the notation used throughout this paper.

3.1. Gilbert-Pollak Conjecture and Steiner Tree

We begin by formally defining the Minimum Spanning Tree and the Steiner Minimal Tree.

Minimum Spanning Tree & Steiner Minimal Tree

Definition 1 (Minimum Spanning Tree). Consider a set V of n points in the Euclidean plane \mathbb{R}^2 . A spanning tree on V is a connected, acyclic graph with vertex set V . When the length of each edge is defined as the Euclidean distance between its endpoints, a spanning tree that minimizes the total length is called a Minimum Spanning Tree.

Definition 2 (Steiner Minimal Tree). Consider a set V of n points in the Euclidean plane. The shortest network interconnecting all points in V , where the length of each edge is measured by Euclidean distance, is necessarily a tree, referred to as a Steiner Minimal Tree. A Steiner Minimal Tree may contain auxiliary vertices not in V . These additional vertices are called Steiner points, while the points in V are referred to as regular points.

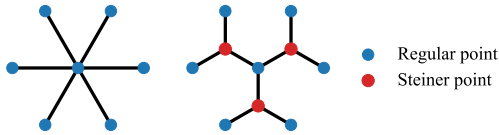


Figure 3. Illustration of minimum spanning tree (left) and Steiner minimal tree (right).

Based on the definitions of Minimum Spanning Tree and Steiner Minimal Tree, we formally define the Steiner ratio and verbalize Gilbert-Pollak Conjecture as follows:

Steiner Ratio and Gilbert-Pollak Conjecture

Definition 3 (Steiner Ratio). The Steiner ratio is defined as the infimum of the ratio of the length of the Steiner Minimal Tree to the length of the Euclidean

Minimum Spanning Tree over all finite sets of points V :

$$\rho_{\text{Steiner}} = \inf_V L_S(V)/L_m(V),$$

where $L_S(V)$ and $L_m(V)$ denote the lengths of Steiner Minimal Tree and Minimum Spanning Tree, respectively.

Conjecture (Gilbert-Pollak). Gilbert & Pollak (1968) famously conjectured that this ratio is lower-bounded by: $\rho_{\text{Steiner}} = \sqrt{3}/2 \approx 0.866$.

Progress on the Steiner Ratio Lower Bound. Gilbert & Pollak (1968) originally conjectured that $\rho_{\text{Steiner}} = \sqrt{3}/2$. Given the intractability of a direct proof, extensive research has historically focused on tightening the lower bound. This bound was successively improved from an initial 0.5 (Moore, as reported in Gilbert & Pollak (1968)) to 0.577 (Graham & Hwang, 1976), 0.743 (Chung & Hwang, 1978), 0.8 (Du & Hwang, 1983), and finally 0.824 (Chung & Graham, 1985). Remarkably, however, progress has stalled entirely since 1985. The primary obstacle lies in the combinatorial explosion of topological structures required for analysis, which far exceeds the capacity of human derivation.

3.2. Mathematical Framework for Proving Steiner Ratio Lower Bound

In this section, we briefly describe the mathematical framework for proving lower bound for Steiner ratio. Many of the mathematical details can be found in Appendix A.1.1.

We first give a very brief and informal description. The framework for establishing the Steiner ratio lower bound is mathematical induction. Assuming that for any set of points with cardinality at most $n - 1$, the Steiner ratio is lower-bounded by ρ . To extend this to a set V of n points, the core strategy involves a reduction argument: identifying a specific subset $V' \subset V$ of size $n - r$ (where $r \geq 1$) such that the marginal gain in the Steiner tree length satisfies $\Delta L_S / \Delta L_m \geq \rho$. Here, $\Delta L_S = L_S(V) - L_S(V')$ and $\Delta L_m = L_m(V) - L_m(V')$ denote the reduction in the lengths of the Steiner Minimal Tree and the Minimum Spanning Tree, respectively. Since $|V'| \leq n - 1$, the inductive hypothesis guarantees $L_S(V')/L_m(V') \geq \rho$. Combining

this with the marginal condition $\Delta L_S \geq \rho \Delta L_m$ completes the inductive step, proving $L_S(V)/L_m(V) \geq \rho$.

However, executing this reduction presents two formidable challenges: (1) Combinatorial Search: Identifying the optimal subset V' —specifically, determining the reduction size r (e.g., reducing to $n - 1$, $n - 2$, etc.) and selecting the exact points—requires searching a vast combinatorial space. (2) Geometric Verification: For a chosen V' , proving the inequality $\Delta L_S \geq \rho \Delta L_m$ is non-trivial. It necessitates formulating novel geometric theorems and analyzing complex functional properties, such as monotonicity and extremal values over high-dimensional continuous domains.

Throughout the sequence of previous works on the lower bound, the complexity of these geometric constructions and functional analyzes has progressively escalated, eventually exceeding the limits of manual tractability. This intractability motivates our introduction of an LLM-based system to automate the discovery process.

We now present the precise mathematical framework. The crux of the induction method is to **prune** some regular points $V^* \subsetneq V$ from the SMT by performing certain operations, thereby reducing the problem size to $V' = V \setminus V^*$. The key is to prove that the Steiner ratio ρ can still be maintained during these operations.

The pruning operation can be summarized into three steps: (1) *Steiner Tree Pruning*: Remove a subset of edges S^- from the SMT such that V^* becomes disconnected from the rest. (2) *Spanning Tree Connection*: Restore connectivity between V^* and the remaining points by adding a set of edges t^* between regular points, which can be viewed as part of a spanning tree. (3) *Steiner Tree Reconstruction*: Connect the remaining points using a new Steiner tree S^+ , thereby forming a complete Steiner tree.

In this pruning process, the decrease in the Steiner tree length is given by $\Delta L_S = L_{S^-} - L_{S^+}$, while the increase in the spanning tree length is given by $\Delta L_m = L_{t^*}$. Here, L_X denotes the total edge length of graph X . The requirement for the induction to hold is that $\Delta L_S / \Delta L_m \geq \rho$, which is equivalent to $\rho \cdot L_{t^*} + L_{S^+} - L_{S^-} \leq 0$. If this condition holds, then combining it with the inductive hypothesis $L_S(V')/L_m(V') \geq \rho$ allows us to derive $L_S(V)/L_m(V) \geq \rho$, thereby completing the induction step. Therefore, we can reformulate the verification of a candidate lower bound ρ for the Steiner ratio as a minimax condition as Theorem 4. In the following

sections, we introduce an LLM-based mathematical framework designed to address this minimax problem.

Sufficient Condition for Lower Bound

Theorem 4. *Let \mathcal{W} denote the space of all edge-length vectors associated with the tree topology. For any choice of splitting $\tau = (V^*, S^-, S^+, t^*)$ and geometric configuration $w \in \mathcal{W}$, we define the splitting function $F_\tau(w, \rho)$ as:*

$$F_\tau(w, \rho) = \rho \cdot L_{t^*} + L_{S^+} - L_{S^-}.$$

Let \mathcal{F} be a family of functions corresponding to admissible splits τ , which we denote as splitting function. The lower bound $\rho_{\text{Steiner}} \geq \rho$ is established if:

$$\max_{w \in \mathcal{W}} \min_{F \in \mathcal{F}} F(w, \rho) \leq 0. \quad (1)$$

We say that a value ρ is feasible if the condition equation 1 holds.

4. LLM Math System for the Conjecture

To effectively leverage LLMs for the Gilbert-Pollak Conjecture, we must systematically address three fundamental challenges: (1) **Search Space**. Spanning graph theory and computational geometry, the conjecture entails a search space far larger than that of contest-level mathematics, leading to severe hallucinations when LLMs are applied naïvely. We therefore need to construct a compact search space that constrains LLMs to generate reasonable reasoning trajectories with high probability. (2) **Rigorous Verification**. We require the system to produce correct derivations and rigorously verified lower bounds, which serve as a quantitative reward for evaluating the LLM’s generations. (3) **Iterative Reflection**. As demonstrated by recent advances like DeepSeek-R1 (Guo et al., 2025), reflection plays a critical role in solving complex problems. We therefore need to build a mechanism designed to identify bottlenecks in intermediate outputs, enabling the model to reflect and iteratively refine its reasoning to obtain improved results.

To address these challenges, we first introduce a class of *verification functions* and theoretically show that, given a suitable collection, the corresponding lower bound can be computed efficiently. Consequently, obtaining improved bounds is equivalent to constructing richer and more informative valid verification functions, providing a tractable and systematic solution for Challenge (2).

Furthermore, the verification function provides significant structural advantages for leveraging LLMs. Specifically, we show that any verification function can be decomposed into two parameterized lemmas. Rather than tasking the model with solving the conjecture directly, we cast the generation objective as producing rule-constrained implementations of these lemmas, expressed as executable code, which signifi-

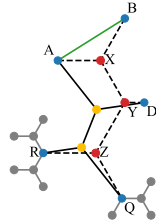


Figure 4. Illustration of Pruning Process. We try to prune $V^* = \{B\}$. Black dashed lines are S^- . Black solid lines are S^+ . Green line is t^* .

cantly simplifies the generation space, thereby effectively addressing Challenge (1).

Finally, we develop a bottleneck region-based reflection mechanism. Leveraging the reward signal and the verification process, we introduce an algorithm that automatically identifies key bottleneck regions limiting further improvements of the lower bound and feeds this information back to the LLM in natural language, guiding subsequent generations to overcome these bottlenecks. Experiments show that this signal significantly improves the effectiveness of LLM, thereby addressing Challenge (3).

Overview & Section Roadmap

An overview of our system is illustrated in Figure 2. In Section 4.1, we begin by formally defining the *verification function* and establishing a method to compute lower bounds based on this formulation. The lower bound serves as the reward model of the system. In Section 4.2, we demonstrate that the search for a verification function is theoretically equivalent to identifying specific classes of lemmas. Leveraging this insight, we design an LLM-driven agent to automatically generate and filter these lemmas. Finally, Section 4.3 details the iterative interaction between the agent and the reward model with a *reflection mechanism*.

4.1. Reward Model

The general objective of the reward in LLM is to evaluate the generated output. In our context, the reward is to determine the tightest lower bound for the Steiner ratio from the “generated proof”. Theorem 4 establishes that the statement “the Steiner ratio is lower bounded by ρ ” is equivalent to verifying that $\max_{\mathbf{w} \in \mathcal{W}} \min_{F \in \mathcal{F}} F(\mathbf{w}, \rho) \leq 0$. However, directly evaluating this continuous-domain minimax problem is computationally intractable.

To make verification tractable, we employ a Branch-and-Bound strategy that recursively partitions the continuous parameter space \mathcal{W} into smaller hyperrectangles, as illustrated in Figure 5 for the 2D case. For each hyperrectangle, our objective is to identify a single function $f \in \mathcal{F}$ that ensures $f(\mathbf{w}) \leq 0$ globally within the subdomain. However, direct verification is infeasible due to the continuous nature of the hyperrectangle. To address this challenge, we introduce verification functions, which serve as upper bounds for the underlying splitting functions while satisfying specific structural

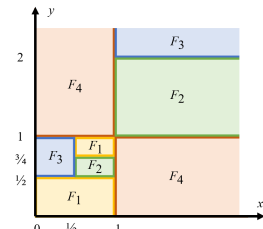


Figure 5. Branch-and-Bound on 2D Plane

constraints. We formally define these functions as follows.

Verification Function

Definition 5. A function $f : \mathcal{W} \rightarrow \mathbb{R} \cup \{+\infty\}$ is called a *verification function* if it satisfies the following two conditions:

1. **Shape Constraint:** The restriction of f to any line parallel to a coordinate axis is unimodal (first non-increasing and then non-decreasing).
2. **Bounding Constraint:** There exists a splitting function $g \in \mathcal{F}$ such that $g(\mathbf{w}) \leq f(\mathbf{w})$, $\forall \mathbf{w} \in \mathcal{W}$.

We denote the set of all verification functions by \mathcal{F}_{ver} .

Remark: The central challenge in verifying $f(\mathbf{w}) \leq 0$ throughout each hyperrectangle is that exhaustive pointwise checking is infeasible in a continuous domain. The following theorem addresses this challenge by establishing that the maximum value of our verification function is attained at the vertices. This property effectively reduces the verification problem to a finite set of vertex checks. We now state the theorem as follows:

Vertex Maximum Property

Theorem 6. Let $H \subset \mathcal{W}$ be a bounded axis-aligned hyperrectangle and let f be any function in \mathcal{F}_{ver} . A key property is that the global maximum of f over H is attained at one of its vertices. Consequently, if

$$\max_{\mathbf{w} \in \mathcal{V}(H)} f(\mathbf{w}) \leq 0, \quad (2)$$

then $f(\mathbf{w}) \leq 0$ for all $\mathbf{w} \in H$, which implies that the underlying splitting function $g(\mathbf{w}) \leq 0$.

Leveraging these theoretical properties of the verification function, we construct a reward model to compute the lower bound of the Steiner ratio. We present the core algorithm below, deferring the full pseudocode and detailed explanations to Appendix D.1.

Algorithm for Reward Model. To determine the maximal valid lower bound, the reward model employs a binary search, using a feasibility oracle grounded in Theorem 6. This oracle recursively partitions the continuous parameter space \mathcal{W} into hyperrectangles and certifies each region via the following steps:

- (1) *Region Partitioning.* We recursively partition the infinite parameter space into hyperrectangle regions.
- (2) *Vertex Verification.* For bounded regions, we select a verification function f and invoke the Vertex Maximum Property. By verifying $f(\mathbf{w}) \leq 0$ at all vertices, we mathematically guarantee that the inequality holds for every point \mathbf{w} within the region.
- (3) *Monotonicity Check for Unbounded Regions.* For unbounded regions, we first verify that f is non-increasing along those unbounded dimensions, ensuring the maximum

value occurs at the finite lower boundary (a “slice” of the region). We then apply vertex verification to this bounded slice. Details of the monotonicity check are provided in Appendix B.4. (4) *Refinement via Subdivision*. Unverified regions are subdivided along one dimension into two halves, and recursively attempt verification.

The procedure terminates when either all regions are certified within the region number threshold, in which case the candidate ρ is declared *feasible*, or when the budget is exhausted with remaining uncertified regions, in which case ρ is reported as *infeasible*.

4.2. LLM Agent

Identifying effective verification functions that yield tight lower bounds remains challenging, as it requires deep geometric intuition, creative lemma construction, and careful analysis of function properties. Human mathematicians may struggle to systematically search and explore potentially useful geometric lemmas for this task. To address this challenge, we develop an LLM agent to automate and scale this discovery process.

We demonstrate that finding a verification function reduces to identifying two types of simpler geometric lemmas: (1) the Trapped Regular Point Lemma and (2) the Valid 4-Point Steiner Tree Lemma. (This equivalence is illustrated in Figure 8 and formally proven in Theorem 18, Appendix B.2). Within our framework, the LLM generates candidate lemmas in the form of structured code snippets. This approach significantly simplifies the generation process and facilitates rigorous verification. In the subsequent sections, we detail how we leverage the LLM to discover these lemmas.

4.2.1. FINDING TRAPPED REGULAR POINT LEMMA

In this section, we detail the methodology for discovering Trapped Regular Point Lemmas using LLMs. We define two distinct categories of rules: Type A rules encode necessary properties that any Steiner Minimal Tree (SMT) must satisfy, while Type B rules specify sufficient conditions that guarantee the existence of an implicit regular point. Given the vast combinatorial space of rule interactions—which renders manual exploration intractable (see Appendix F for details)—we employ an LLM integrated with local tools (e.g., Mathematica). By iteratively validating hypotheses, the LLM discovers effective rule combinations and synthesizes conditions that imply regularity. These conditions are subsequently simplified by the model to derive novel geometric lemmas.

Theoretical Foundation. Consider traversing a path on the Steiner tree. At each intermediate Steiner point, we consistently select the branch corresponding to a 60° clockwise turn (“turning right”). This traversal traces a maximal chain

of vertices A_0, A_1, \dots, A_n , where A_n is a regular point and A_1, \dots, A_{n-1} are Steiner points.

Due to the geometric constraints established in Lemma 11, every internal angle $\angle A_{i-1}A_iA_{i+1}$ along this chain is exactly 120° . We abstract this configuration as the **Steiner Spiral Chain**, as illustrated in Figure 6. For analysis, we denote the edge lengths as $a_i = |A_{i-1}A_i|$ for $i = 1, \dots, n$, and normalize the system such that $a_1 = 1$.

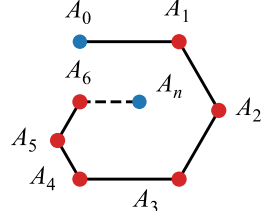


Figure 6. The Steiner Spiral Chain structure

Crucially, this chain is non-intersecting and constitutes the Steiner Minimal Tree for the set of vertices $\{A_0, \dots, A_n\}$. Our goal is to derive conditions under which A_n is trapped inside a bounded polygon. We construct a discrete **Structured Reasoning Space** consisting of axiomatic templates. We formalize the constraints of the Steiner Spiral using two sets of predicates, denoted \mathcal{C}^A and \mathcal{C}^B , which serve as the atomic actions for the LLM agent.

Type A/B Condition

Lemma 7 (Type A: Intrinsic Properties). *For any $0 \leq u < s \leq v \leq n$, the inequality $|A_uA_v| \geq a_s$ (denoted $C_{u,v,s}^A$) is always satisfied.*

Lemma 8 (Type B: Sufficient Trapping Conditions). *For $0 \leq u < s \leq v < \min(6, n)$, let H be the orthogonal projection of A_u onto line A_vA_{v+1} . We define the predicate $C_{u,v,s}^B$ as (1) H lies on ray A_vA_{v+1} and (2) $|A_uH| < a_s$. If $C_{u,v,s}^B$ holds, then A_n is trapped inside the polygon $A_u \dots A_v H A_u$.*

These predicates correspond to algebraic inequalities on \mathbf{w} (e.g., $C_{0,2,1}^B \iff (a_2 \leq 1) \wedge (\sqrt{3}/2 \cdot (1 + a_2) \leq 1)$). Full derivations are in Appendix B.1.

Trapped Regular Point Theorem

Theorem 9. *Let $\{C_i^A\}_{i=1}^k \subseteq \mathcal{C}^A$ and $\{C_j^B\}_{j=1}^l \subseteq \mathcal{C}^B$ be subsets of conditions. Suppose a linear constraint C on \mathbf{w} satisfies the implication: $C \wedge \left(\bigwedge_{i=1}^k C_i^A\right) \implies \bigvee_{j=1}^l C_j^B$. Then, if \mathbf{w} satisfies C , the regular point A_n is trapped inside the corresponding polygonal region.*

LLM-Guided Lemma Generation. This module operationalizes Theorem 9 through the synthesis of valid constraints via an LLM agent. Here, we delineate the process of guiding the LLM to identify trapped regular point lemmas. Comprehensive details are available in Appendix F.

• *Preparation: Geometric Definition.* We begin by providing the LLM with the geometric definition of the coordinate system and the structure of the polygonal chain.

• *Constraint Selection.* Since reasoning over the complete sets \mathcal{C}^A and \mathcal{C}^B is computationally intractable, we supply the LLM with the full sets of Type A and Type B conditions, and task the LLM with selecting a concise subset of relevant conditions (typically 1–3 items). The goal is to identify constraints that collectively enforce the trapping condition.

• *Derivation and Simplification.* The agent first employs Mathematica’s `Reduce` function to compute the feasible region of w that satisfies the implication $\bigwedge C_i^A \implies \bigvee C_j^B$. However, the raw region derived by Mathematica is often complex and non-linear, rendering it incompatible with our reward model. Consequently, we task the LLM with simplifying this region into explicit *linear constraints*, followed by a verification step using Mathematica.

Derivation & Verification Prompt

Step 4.1: Attempt Derivation

Run the following logic in Mathematica using the expressions copied from the list:

```
(* Define the logic: ForAll tail_vars,
(Steiner_Constraints) implies (Trap_Goal) *)
Reduce[
  ForAll[{a5, a6},
    a5 > 0 && a6 > 0 && <Selected_A_Props>,
    <Selected_B_Props>
  ] && a2 > 0 && a3 > 0 && a4 > 0,
  {a2, a3, a4}
]
```

Tip: If the result is non-linear, relax it to a linear inequality that still covers the Box.

Step 4.2: Verification

Verify your derived condition `<Cond>`:

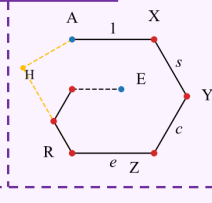
```
Reduce[
  !ForAll[{a5, a6}, a5 > 0 && a6 > 0 &&
  <Selected_A_Props>, <Selected_B_Props>]
  && a2 > 0 && a3 > 0 && a4 > 0 && <Cond>,
  {a2, a3, a4}
]
```

The output MUST be `False`.

• *Coding and Output.* Finally, we instruct LLM to encapsulate the derived constraints into two code snippets: boolean function `X_cond` checks if w satisfies the derived linear constraints, while floating-point function `AX_upper_bound` computes the distance upper bound from A_0 to trapped A_n . Then they are transformed into verification functions and added to \mathcal{F}_{ver} . We present an example of LLM-generated Trapped Regular Point Lemma, accompanied by its corresponding structured code snippet, below.

LLM Generated Trapped Regular Point Lemma

Lemma. If $e < 1 - c + \frac{2}{\sqrt{3}} \cdot s$ and $c + e > 1$, then there exists a regular point E s.t. $|AE| \leq \max \left\{ 1, |AY|, |AZ|, |AR|, \frac{\sqrt{3}}{2} \cdot (c + e - 1) \right\}$.



```
def X_cond(s, c, e) -> bool:
    rhs = 1.0 - c + (2.0 / math.sqrt(3.0)) * s
    return (e < rhs) and (c + e > 1.0)
def AX_upper_bound(s, c, e) -> float:
    dY = math.sqrt(1.0 + s + s*s)
    dZ = math.sqrt(1.0 + s + s*s - c + s*c + c*c)
    dR = math.sqrt(s*s + c*c + s*(1.0+c-e) + c*(e-1.0) +
    (e-1.0)*(e-1.0))
    dH = (c + e - 1.0) * math.sqrt(3.0) / 2.0
    return max(1.0, dY, dZ, dR, dH)
```

4.2.2. FINDING VALID 4-POINT STEINER TREE LEMMA

In this section, we focus on discovering valid 4-point Steiner tree lemmas. Our goal is to identify regions in the parameter space where a specific topology is guaranteed to exist and be computable. Analogous to Section 4.2.1, our core strategy involves constructing a structured reasoning space, within which the LLM performs reasoning and deduction.

Theoretical Foundation. Consider four points A, B, C , and D forming a convex quadrilateral in clockwise order. We focus on the (AB) - (CD) topology, defined as follows:

Steiner Tree Type

Definition 10 (Steiner Tree Type). *The (AB) - (CD) type Steiner tree consists of two Steiner points S and T , and five edges: $(A, S), (B, S), (S, T), (T, C), (T, D)$. The edges incident to each Steiner point meet at 120° angles, as illustrated in Figure 7.*

We adopt the Valid 4-Point Steiner Tree Theorem from Du et al. (1987) to determine the existence of the (AB) - (CD) topology. The theorem’s details are provided in Appendix A.2 as Theorem 14. The LLM agent’s task is to translate the geometric conditions of the theorem into algebraic constraints on the parameter space w , simplifying them to satisfy the orthogonally convex property required by our reward model for subsequent conversion into verification functions.

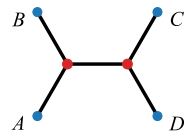
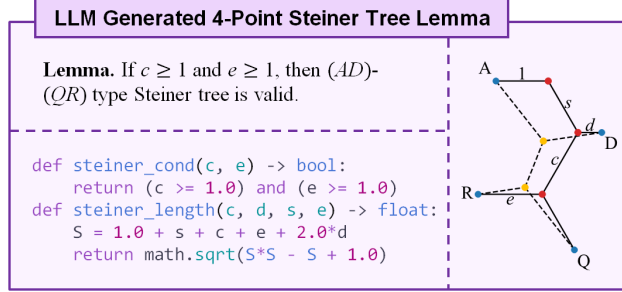


Figure 7. (AB) - (CD) type Steiner tree.

LLM-Guided Lemma Generation. The task of LLM Agent is to transform the existence conditions of the Steiner tree involving four specific points into a form that can be used for verification function. The process proceeds as follows:

- *Translation*: Given a specific set of four terminals, the LLM translates the geometric conditions of Theorem 14 into algebraic constraints on the parameters w .
- *Simplification*: Following the translation step, the resulting raw algebraic constraints are often complex and non-convex. To address this, the LLM performs a heuristic simplification to identify a tractable constraint set that implies the original complex conditions.
- *Verification*: Finally, the LLM must verify that the resulting condition is *orthogonally convex* and implies the validity conditions. Upon validation, new verification functions with S^+ being the specific topology will be added to \mathcal{F}_{ver} .
- *Coding and Output*: The LLM is instructed to encapsulate the derived constraints into two code snippets: boolean function `steiner_cond` checks if w satisfies the derived constraints, while floating-point function `steiner_length` computes the 4-point Steiner tree length. Then they are transformed into verification functions and added to \mathcal{F}_{ver} . We present an example of an LLM-generated 4-Point Steiner Tree Lemma, accompanied by its corresponding structured code snippet, below.



4.3. Iterative Process

In this subsection, we describe the iterative closed-loop interaction between the LLM Agent and the reward model. While self-reflection mechanisms have proven pivotal in solving contest(Jaech et al., 2024; Singh et al., 2025; Lai et al., 2025)-level math problems—enabling models to review generation history, detect errors, and iteratively refine accuracy—they are not directly applicable here. In our system, the objective is not to solve the Gilbert-Pollak conjecture directly, but to synthesize intermediate lemmas. Consequently, generic reflection strategies are insufficient. Instead, we design a targeted supervisory signal that explicitly identifies areas for improvement, guiding the LLM to overcome specific bottlenecks during the refinement process.

Once the LLM generates lemmas, they are converted into verification functions to compute the current lower bound. To iteratively tighten this bound, the reward model attempts to certify an incremented candidate $\rho + \delta$. If the verifica-

tion process fails, leaving a set of uncertified subregions $\{B_1, \dots, B_k\}$, the model performs a geometric abstraction by computing the minimal axis-aligned hyperrectangle B^* that encloses them. We refer to B^* as the bottleneck region. This region is converted into a structured prompt by explicitly providing the LLM with the coordinate intervals of each dimension in B^* . Consequently, the LLM is instructed to generate lemmas specifically targeting this region, thereby enabling the construction of new verification functions to close the gap. We now formally describe the entire iterative process incorporating this bottleneck reflection mechanism.

- **Evaluate.** The reward model evaluates the feasible lower bound using the current set of verification functions.
- **Reflection.** A bottleneck region is extracted from the verification process and fed back to the LLM Agent.
- **Propose.** Guided by the current bottleneck region, the LLM Agent proposes new lemmas targeting the limiting part of the parameter space to overcome the current optimization bottleneck.
- **Translate.** After the proposed lemmas are manually validated for correctness, they are translated into verification functions that can be consumed by the reward model, resulting in an augmented set of verification functions.

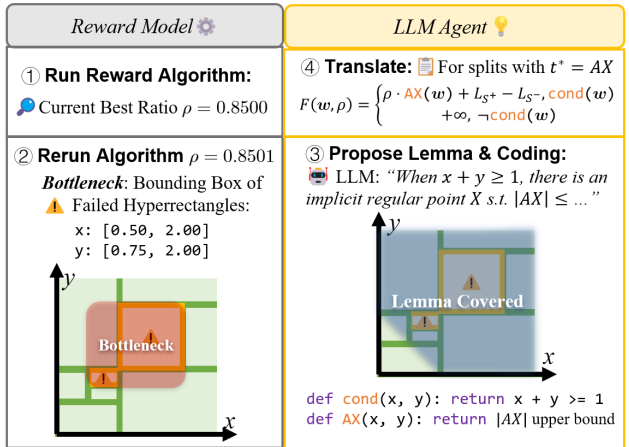


Figure 8. Interaction Between Reward Model & LLM Agent

Verification of the Proof Correctness. We ensure the reliability of our results through a dual-verification strategy. First, the LLM acts solely as a reasoning engine, offloading all validation tasks to Mathematica to perform exact computation. This significantly reduces hallucinations in the generated lemmas. Second, we performed independent manual verification of the generated proofs to confirm that the overall logical argument is sound. Consequently, the final lower bound is a standard mathematical proof that stands independent of the generative AI pipeline.

5. Experiments and Results

We evaluate our system along several key dimensions: lemma quality, robustness across different LLM backbones, the role of reflection in iterative reasoning, and the final improvement of the Steiner ratio lower bound.

Lemma Quality. Across approximately 100 rounds of experiments, more than 80% of LLM-proposed lemmas are effective when instantiated as verification functions. This high success rate highlights the advantages of operating within *narrow reasoning spaces* and using a *localized, lemma-driven approach*, rather than attempting end-to-end optimization over the full parameter space.

Robustness Across LLM Backbones. We conducted experiments using GPT-5 and Gemini 3 Pro. In all cases, the LLMs successfully proposed valid lemmas, and after roughly a dozen iterative rounds, the system consistently converged to a Steiner ratio lower bound of approximately 0.855. These results demonstrate that the framework is robust and largely insensitive to the choice of LLM backbone.

Reflection Ablation. To evaluate the importance of the reflection mechanism, we performed ablation experiments where the reflection bottleneck was removed. In this setting, the system failed to improve the lower bound over 10 iterative rounds, confirming that reflection is essential for guiding lemma discovery and enabling improvement.



Figure 9. Illustration of the ratio change throughout the iteration over steps and comparison with SOTA result of previous works.

Typical Trajectory and Final Result. Figure 9 summarize a representative trajectory of the system. Through iterative interaction between the LLM agent and the reward model, the lower bound progressively improves and stabilizes at 0.8559. Importantly, this bound has been rigorously verified across the entire parameter space, and all lemmas proposed along this trajectory have been manually checked for correctness, ensuring the validity of the overall proof independent of the specific generative AI pipeline. Across this trajectory, the LLM consumed approximately 0.5M tokens ($\sim 35K$ per

round) and 4.6 hours of reasoning, while computations of the reward model required roughly 11.7 hours. The detailed content of each step of improvement can be found in the Appendix C.

6. Conclusion

We present an LLM-based system designed to advance the Gilbert-Pollak Conjecture. By guiding the LLM to generate structured geometric lemmas and instantiating them as verification functions, the system iteratively refines its reasoning in a localized search space, producing a significant improvement over the previous lower bound for the Steiner ratio. Our experiments demonstrate that this approach is robust across different LLM backbones and relies on only a modest number of model calls, highlighting its potential as a scalable paradigm for leveraging LLMs in math research.

Impact Statement

This paper presents work whose goal is to advance the field of machine learning. There are many potential societal consequences of our work, none of which we feel must be specifically highlighted here.

References

Achim, T., Best, A., Bietti, A., Der, K., Fédérico, M., Gukov, S., Halpern-Leistner, D., Henningsgard, K., Kudryashov, Y., Meiburg, A., et al. Aristotle: Imo-level automated theorem proving, 2025. *URL https://arxiv.org/abs/2510.01346*.

Chen, J., Chen, W., Du, J., Hu, J., Jiang, Z., Jie, A., Jin, X., Jin, X., Li, C., Shi, W., et al. Seed-prover 1.5: Mastering undergraduate-level theorem proving via learning from experience. *arXiv preprint arXiv:2512.17260*, 2025.

Chervonyi, Y., Trinh, T. H., Olšák, M., Yang, X., Nguyen, H., Menegali, M., Jung, J., Verma, V., Le, Q. V., and Luong, T. Gold-medalist performance in solving olympiad geometry with alphageometry2. *arXiv preprint arXiv:2502.03544*, 2025.

Chung, F. and Hwang, F. A lower bound for the steiner tree problem. *SIAM Journal on Applied Mathematics*, 34(1): 27–36, 1978.

Chung, F. R. and Graham, R. L. A new bound for euclidean steiner minimal trees. *Annals of the New York Academy of Sciences*, 440(1):328–346, 1985.

Du, D. and Hu, X. *Steiner tree problems in computer communication networks*. World Scientific, 2008.

Du, D.-Z. and Hwang, F. K. A new bound for the steiner

ratio. *Transactions of the American Mathematical Society*, 278(1):137–148, 1983.

Du, D.-Z., Hwang, F. K., and Yao, E. The steiner ratio conjecture is true for five points. *Journal of Combinatorial Theory, Series A*, 38(2):230–240, 1985.

Du, D. Z., Hwang, F. K., Song, G. D., and Ting, G. Y. Steiner minimal trees on sets of four points. *Discrete & Computational Geometry*, 2:401–414, 1987.

Fawzi, A., Balog, M., Huang, A., Hubert, T., Romera-Paredes, B., Barekatain, M., Novikov, A., R. Ruiz, F. J., Schrittweiser, J., Swirszcz, G., et al. Discovering faster matrix multiplication algorithms with reinforcement learning. *Nature*, 610(7930):47–53, 2022.

Gilbert, E. N. and Pollak, H. O. Steiner minimal trees. *SIAM Journal on Applied Mathematics*, 16(1):1–29, 1968.

Google DeepMind. Ai achieves silver-medal standard solving International Mathematical Olympiad problems, 2024. URL <https://deepmind.google/discover/blog/ai-solves-imo-problems-at-silver-medal-level>. Accessed: 2025-12-26.

Graham, R. L. and Hwang, F. K. Remarks on steiner minimal trees. *Bull. Inst. Math. Acad. Sinica*, 4(1):177–182, 1976.

Guo, D., Yang, D., Zhang, H., Song, J., Zhang, R., Xu, R., Zhu, Q., Ma, S., Wang, P., Bi, X., et al. Deepseek-r1: Incentivizing reasoning capability in llms via reinforcement learning. *arXiv preprint arXiv:2501.12948*, 2025.

Jaech, A., Kalai, A., Lerer, A., Richardson, A., El-Kishky, A., Low, A., Helyar, A., Madry, A., Beutel, A., Carney, A., et al. Openai o1 system card. *arXiv preprint arXiv:2412.16720*, 2024.

Jumper, J., Evans, R., Pritzel, A., Green, T., Figurnov, M., Tunyasuvunakool, K., Ronneberger, O., Bates, R., Žídek, A., Bridgland, A., et al. Alphafold 2. *Fourteenth Critical Assessment of Techniques for Protein Structure Prediction*, pp. 13, 2020.

Jumper, J., Evans, R., Pritzel, A., Green, T., Figurnov, M., Ronneberger, O., Tunyasuvunakool, K., Bates, R., Žídek, A., Potapenko, A., et al. Highly accurate protein structure prediction with alphafold. *nature*, 596(7873):583–589, 2021.

Kahng, A. B. and Robins, G. *On optimal interconnections for VLSI*, volume 301. Springer Science & Business Media, 1994.

Krokidis, M. G., Koumadorakis, D. E., Lazaros, K., Ivantsik, O., Exarchos, T. P., Vrahatis, A. G., Kotsiantis, S., and Vlamos, P. Alphafold3: an overview of applications and performance insights. *International Journal of Molecular Sciences*, 26(8):3671, 2025.

Lai, X., Li, J., Li, W., Liu, T., Li, T., and Zhao, H. Mini-o3: Scaling up reasoning patterns and interaction turns for visual search. *arXiv preprint arXiv:2509.07969*, 2025.

Lam, R., Sanchez-Gonzalez, A., Willson, M., Wirnsberger, P., Fortunato, M., Alet, F., Ravuri, S., Ewalds, T., Eaton-Rosen, Z., Hu, W., et al. Learning skillful medium-range global weather forecasting. *Science*, 382(6677):1416–1421, 2023.

Lample, G., Lacroix, T., Lachaux, M.-A., Rodriguez, A., Hayat, A., Lavril, T., Ebner, G., and Martinet, X. Hyper-tree proof search for neural theorem proving. *Advances in neural information processing systems*, 35:26337–26349, 2022.

Lin, Y., Tang, S., Lyu, B., Wu, J., Lin, H., Yang, K., Li, J., Xia, M., Chen, D., Arora, S., et al. Goedel-prover: A frontier model for open-source automated theorem proving. *arXiv preprint arXiv:2502.07640*, 2025a.

Lin, Y., Tang, S., Lyu, B., Yang, Z., Chung, J.-H., Zhao, H., Jiang, L., Geng, Y., Ge, J., Sun, J., et al. Goedel-prover-v2: Scaling formal theorem proving with scaffolded data synthesis and self-correction. *arXiv preprint arXiv:2508.03613*, 2025b.

Lu, C., Lu, C., Lange, R. T., Foerster, J., Clune, J., and Ha, D. The ai scientist: Towards fully automated open-ended scientific discovery. *arXiv preprint arXiv:2408.06292*, 2024.

Merchant, A., Batzner, S., Schoenholz, S. S., Aykol, M., Cheon, G., and Cubuk, E. D. Scaling deep learning for materials discovery. *Nature*, 624(7990):80–85, 2023.

Pollak, H. O. Some remarks on the steiner problem. *Journal of combinatorial theory, series A*, 24(3):278–295, 1978.

Rubenstein, J. and Thomas, D. A. The steiner ratio conjecture for six points. *Journal of Combinatorial Theory Series A*, 58(1):54–77, 1991.

Singh, A., Fry, A., Perelman, A., Tart, A., Ganesh, A., El-Kishky, A., McLaughlin, A., Low, A., Ostrow, A., Ananthram, A., et al. Openai gpt-5 system card. *arXiv preprint arXiv:2601.03267*, 2025.

Trinh, T. H., Wu, Y., Le, Q. V., He, H., and Luong, T. Solving olympiad geometry without human demonstrations. *Nature*, 625(7995):476–482, 2024.

Xin, H., Guo, D., Shao, Z., Ren, Z., Zhu, Q., Liu, B., Ruan, C., Li, W., and Liang, X. Deepseek-prover: Advancing theorem proving in llms through large-scale synthetic data. *arXiv preprint arXiv:2405.14333*, 2024a.

Xin, H., Ren, Z., Song, J., Shao, Z., Zhao, W., Wang, H., Liu, B., Zhang, L., and Lu, X. Qiushi du, et al. deepseek-prover-v1. 5: Harnessing proof assistant feedback for reinforcement learning and monte-carlo tree search. *arXiv preprint arXiv:2408.08152*, 3, 2024b.

Yamada, Y., Lange, R. T., Lu, C., Hu, S., Lu, C., Foerster, J., Clune, J., and Ha, D. The ai scientist-v2: Workshop-level automated scientific discovery via agentic tree search. *arXiv preprint arXiv:2504.08066*, 2025.

Yang, K., Swope, A., Gu, A., Chalamala, R., Song, P., Yu, S., Godil, S., Prenger, R. J., and Anandkumar, A. Leandojo: Theorem proving with retrieval-augmented language models. *Advances in Neural Information Processing Systems*, 36:21573–21612, 2023.

Ying, H. et al. Internlm-math: Open math large language models toward verifying reasoning steps. *arXiv preprint arXiv:2402.06332*, 2024.

Appendix

Contents

| | |
|--|-----------|
| A Mathematical Preliminaries | 13 |
| A.1 Background on the Gilbert-Pollak Conjecture | 13 |
| A.1.1 Basic Properties of Steiner Minimal Tree | 13 |
| A.1.2 Core Lemmas | 13 |
| A.2 Geometric Properties of 4-Point Steiner Trees | 14 |
| B Our Theoretical Contributions | 16 |
| B.1 The Type A and B Predicate Framework | 16 |
| B.2 Proof of Theorems in Section 4 | 18 |
| B.3 Proof of Convexity for Splitting Functions | 21 |
| B.3.1 Linearity of L_{S^-} | 21 |
| B.3.2 Convexity of L_{t^*} | 21 |
| B.3.3 Convexity of L_{S^+} for $ S^+ \leq 3$ | 21 |
| B.3.4 Conclusion | 22 |
| B.4 Theoretical Foundation for the Monotonicity Check | 22 |
| B.4.1 Geometric Foundations | 22 |
| B.4.2 Special Analysis on the Monotonicity of f | 23 |
| B.5 Correctness Proof for Algorithm 2 | 23 |
| C Proofs of LLM-Generated Lemmas | 24 |
| D Algorithms and Implementation Details | 32 |
| D.1 Detail Algorithm for Reward Model | 32 |
| D.2 Monotonicity Verification Algorithm | 33 |
| D.3 Strategies for Handling Complex Splits | 33 |
| D.3.1 Methods for Handling Splits with Implicit Regular Points | 33 |
| D.3.2 Methods for Handling Splits with 4-Point Steiner Tree | 33 |
| D.4 Enumeration of Valid Splits | 34 |
| E Experimental Setup and Additional Results | 35 |
| E.1 Baseline Verification Functions | 35 |
| E.2 Problem Decomposition and Search Space Reduction | 36 |
| F LLM Agent and Prompts | 38 |
| F.1 Prompt for Searching Trapped Regular Point Lemmas | 38 |
| F.2 Prompt for Searching Valid 4-Point Steiner Tree Lemmas | 42 |

A. Mathematical Preliminaries

A.1. Background on the Gilbert-Pollak Conjecture

A.1.1. BASIC PROPERTIES OF STEINER MINIMAL TREE

Let V be a finite set of points in the Euclidean plane. We denote the lengths of the Steiner Minimal Tree (SMT) and the Minimum Spanning Tree (MST) on V as $L_S(V)$ and $L_m(V)$, respectively. For an arbitrary geometric graph G , let L_G denote the sum of the Euclidean lengths of its edges. We first recall fundamental geometric properties of SMTs.

Properties of Steiner Minimal Trees

Lemma 11. *Let S be a Steiner Minimal Tree for a set V . The following properties hold:*

1. *Every Steiner point in S has a degree of exactly 3, and the three incident edges meet at 120° angles.*
2. *If $|V| = n$, then S contains at most $n - 2$ Steiner points. A tree with exactly $n - 2$ Steiner points is called a Full Steiner Tree (FST).*
3. *Any SMT can be decomposed into a union of edge-disjoint Full Steiner Trees. Consequently, it suffices to consider only Full Steiner Trees when proving lower bounds on the Steiner ratio.*

Based on Lemma 11, we restrict our analysis to Full Steiner Trees without loss of generality. A defining topological feature of a Full Steiner Tree is that all regular points (terminals) are leaves with a degree of 1. We use **induction** to establish the lower bound. The base case where $|V| \leq 4$ is shown by [Pollak \(1978\)](#). Thus, we may assume $|V| \geq 5$.

Let V be the set of regular points, and let S be $SMT(V)$. To complete the induction step, we focus on a terminal substructure of S . Consider a leaf A of maximum depth in S . Let X be the parent of A . Since A is at maximum depth, the sibling of A must also be a terminal, denoted as B . Let Y be the parent of X . The sibling component D incident to Y cannot have a height exceeding that of X ; consequently, D is necessarily either a single terminal or a Steiner point connected to two terminals.

This results in the two cases illustrated in Figure 10: in the left case, D is a single regular point; in the right case, D is a Steiner point connecting two regular points, U and V . The notations (R) and (Q) denote the residual subtrees connected to the main structure at nodes R and Q . The labels on the edges denote their Euclidean lengths. Because the Steiner ratio is scale-invariant, we normalize the scale of the tree such that the edge AX has length 1 ($|AX| = 1$).

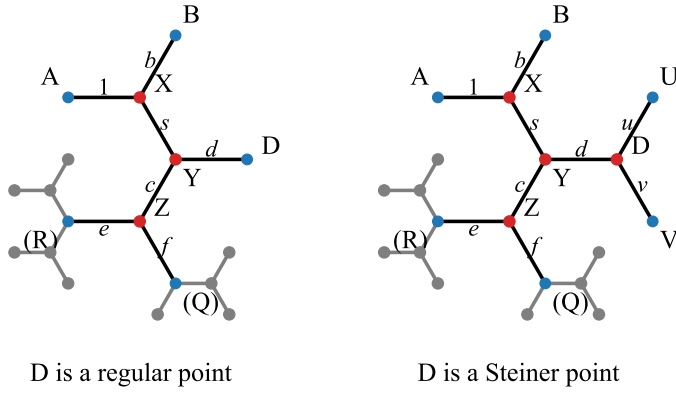


Figure 10. Local substructures of a Steiner Minimal Tree.

A.1.2. CORE LEMMAS

In this section, We will provide a more detailed description of how induction works.

To complete the induction step, we utilize a reduction argument introduced by [Du & Hwang \(1983\)](#).

Du & Hwang (1983) Lemma 3

Lemma 12 (Du & Hwang (1983) Lemma 3). *Let $S = \text{SMT}(V)$ be the Steiner Minimal Tree for a set V of n points. Consider a partition of the edges of S into two disjoint sets, S^- and S_{rem} (where $S_{\text{rem}} = S \setminus S^-$). Let $V^* \subsetneq V$ be a non-empty subset of regular points such that no point in V^* is incident to S_{rem} . We define two auxiliary graphs:*

- t^* : A forest interconnecting V^* and $V \setminus V^*$ using only vertices in V . It must satisfy: (1) For every $x \in V^*$, there exists a path in t^* connecting x to some $y \in V \setminus V^*$. (2) There are no paths in t^* connecting any two distinct points $y_1, y_2 \in V \setminus V^*$.
- S^+ : A graph (may contain auxiliary vertices not in V) such that $S^+ \cup S_{\text{rem}}$ forms a valid Steiner tree (not necessarily minimal) for $V \setminus V^*$.

Inductive Step: Suppose that for all point sets with fewer than n points, the Steiner ratio is at least ρ' . If there exists a tuple (V^*, S^-, S^+, t^*) satisfying $(L_{S^-} - L_{S^+})/L_{t^*} \geq \rho'$, then the Steiner ratio for V also satisfies $L_S(V)/L_m(V) \geq \rho'$.

Intuitively, the constraint on t^* guarantees that any spanning tree of $V \setminus V^*$ combined with t^* yields a spanning tree of V .

Based on Lemma 12, we reformulate the verification of a candidate lower bound ρ for the Steiner ratio as a minimax condition. Let \mathcal{W} denote the space of all edge-length vectors associated with the tree topology shown in Figure 10 ($\mathbf{w} \in \mathcal{W}$ is something like (b, c, d, s, \dots)).

Sufficient Condition for the Steiner Ratio Lower Bound

Corollary 13 (Theorem 4 restated). *For any choice of splitting $\tau = (V^*, S^-, S^+, t^*)$ and geometric configuration $\mathbf{w} \in \mathcal{W}$, we define the splitting function $F_\tau(\mathbf{w}, \rho)$ as:*

$$F_\tau(\mathbf{w}, \rho) = \rho \cdot L_{t^*} + L_{S^+} - L_{S^-}.$$

Let \mathcal{F} be a family of functions corresponding to admissible splits τ . The lower bound $\rho_{\text{Steiner}} \geq \rho$ is established if:

$$\max_{\mathbf{w} \in \mathcal{W}} \min_{F \in \mathcal{F}} F(\mathbf{w}, \rho) \leq 0. \quad (3)$$

We say that a value ρ is feasible if the condition equation 3 holds.

Intuitively, equation 3 states that for any possible geometric configuration of the tree ($\max_{\mathbf{w}}$), there must exist at least one valid strategy for splitting the tree (\min_F) such that the splitting function is non-positive.

A.2. Geometric Properties of 4-Point Steiner Trees

Let U be the vertex of an equilateral triangle $\triangle ABU$ constructed such that A, B, U appear in counterclockwise order. Similarly, let V be the vertex of an equilateral triangle $\triangle CDV$ constructed such that C, D, V appear in counterclockwise order. The existence of the (AB) - (CD) topology is governed by the following conditions:

Valid 4-Point Steiner Tree Theorem

Theorem 14 (Du et al. (1987) Theorem 6). *We say an (AB) - (CD) type Steiner tree is valid if (1) A, B, C and D form a convex quadrilateral. (2) $\max(\angle UCD, \angle UDC, \angle VAB, \angle VBA) \leq 120^\circ$. (3) The intersection angle of the diagonals, $\angle AOB$, is at most 120° , where O is the intersection of AC and BD .*

When these conditions are met, the length of the tree follows a concise formula:

Length of the (AB) - (CD) Type Steiner Tree

Lemma 15. *The length of the (AB) - (CD) type Steiner tree is precisely given by $|UV|$, where U denote the position of point B after segment AB is rotated counterclockwise 60° about point A and V denote the position of point D after segment CD is rotated counterclockwise 60° about point C .*

Proof. By construction, points A, U, B are arranged in counterclockwise order and form an equilateral triangle, as are

points C, V, D . Consequently, $\triangle ABU$ and $\triangle CVU$ are equilateral triangles.

Recall Definition 10. A key property of the geometry is that the angle between the segments connecting to the non-bridge endpoints at a Steiner point is 120° . Therefore, we note that $\angle ASB = 2\pi/3$. Since $\triangle ABU$ is equilateral, $\angle AUB = \pi/3$. The sum of these opposite angles in the quadrilateral $AUBS$ is $\angle ASB + \angle AUB = 2\pi/3 + \pi/3 = \pi$. This implies that the points A, U, B, S are concyclic.

Since the points are concyclic, the angle $\angle ASU$ subtends the same arc AU as the angle $\angle ABU$. Thus, $\angle ASU = \angle ABU = \pi/3$. From the definition of the Steiner point S , the segments SA, SB , and ST form 120° angles. Specifically, $\angle AST = 2\pi/3$. It follows that $\angle ASU + \angle AST = \pi/3 + 2\pi/3 = \pi$, which proves that the points U, S, T are collinear. By a similar argument for the points C, V, D, T , we can show that V, T, S are also collinear. Combining these results, we conclude that the four points U, S, T, V lie on a single straight line in that order.

Applying Ptolemy's theorem to the cyclic quadrilateral $AUBS$, we have:

$$|AB| \cdot |US| = |AU| \cdot |BS| + |BU| \cdot |AS|.$$

Since $\triangle ABU$ is equilateral, $|AU| = |BU| = |AB|$. Substituting these into the equation and dividing by $|AB|$ yields:

$$|US| = |AS| + |BS|.$$

Similarly, applying Ptolemy's theorem to the cyclic quadrilateral $CVDT$, we obtain:

$$|VT| = |CT| + |DT|.$$

As the points U, S, T, V are collinear, the length of the segment $|UV|$ is the sum of the lengths of the constituent segments:

$$|UV| = |US| + |ST| + |TV| = (|AS| + |BS|) + |ST| + (|CT| + |DT|).$$

This sum is precisely the total length of the edges in the (AB) - (CD) type Steiner tree. \square

B. Our Theoretical Contributions

This appendix consolidates the original theoretical contributions of our work. Our primary objective is to elaborate on how we transform the computationally intractable minimax problem $\max_w \min_F F(w, \rho) \leq 0$ (from Theorem 4 of the main text) into a mathematically rigorous and tractable verification pipeline.

B.1. The Type A and B Predicate Framework

Type A and B Predicate Framework

Lemma 7 (restated). *For any $0 \leq u < s \leq v \leq n$, $|A_u A_v| \geq a_s$.*

Proof. We prove the lemma by contradiction. Assume for the sake of contradiction that $|A_u A_v| < a_s$. We can then construct a new Steiner tree by removing the edge $A_s A_{s-1}$ from the original tree and adding the edge $A_u A_v$. This operation results in a new, valid Steiner tree whose total length is less than that of the original, since an edge of length a_s was replaced by one of length $|A_u A_v|$. This contradicts the assumption that the original tree is a minimal Steiner tree. \square

Lemma 8 (restated). *For any $0 \leq u < s \leq v < \min(6, n)$, let H be the foot of the perpendicular from A_u to line $A_v A_{v+1}$. If H lies on the ray $A_v A_{v+1}$ and $|A_u H| < a_s$, then A_n will be trapped inside polygon $A_u A_{u+1} \dots A_v H A_u$.*

Proof. First, we need to prove a more specific form of this lemma. To this end, we introduce the following lemma:

Type A and B Predicate Framework

Lemma 16. *Consider a simple polygonal chain $X_1 X_2 \dots X_n$ in the plane, formed by n segments connected end-to-end, satisfying the following conditions:*

1. *The angle between any two consecutive segments $X_i X_{i+1}$ and $X_{i+1} X_{i+2}$ is 120° .*
2. *When traversing the chain in the order X_1, X_2, \dots, X_n , every turn at each vertex X_i is a right turn.*

If $n \geq 7$ and the ray starting from X_6 through X_7 intersects one of the segments $X_1 X_2, X_2 X_3, \dots, X_4 X_5$, then all subsequent vertices X_7, X_8, \dots, X_n lie within the closed region Ω enclosed by the segments $X_1 X_2, X_2 X_3, X_3 X_4, X_4 X_5, X_5 X_6$ and the line passing through X_6 and X_1 .

Proof. We establish a complex coordinate system by setting the segment $X_1 X_2$ on the real axis. Let each point X_i be represented by its corresponding complex number, also denoted by X_i .

The vector from X_i to X_{i+1} can be expressed as $X_{i+1} - X_i$. Due to the right-turn condition, each subsequent vector is rotated. This gives us the relation:

$$X_{i+1} - X_i = \lambda_i \cdot \varepsilon^{i-1},$$

where $\varepsilon = e^{-\pi i/3}$ represents a 120° right turn, and $\lambda_i > 0$ is the length of the segment $|X_i X_{i+1}|$.

From this, the position of any vertex X_i can be written as a sum:

$$X_i = X_1 + \sum_{k=1}^{i-1} \lambda_k \varepsilon^{k-1}.$$

Based on this formula, in conjunction with the condition that the ray $X_6 X_7$ intersects one of the segments in the initial chain $\{X_1 X_2, \dots, X_4 X_5\}$, we can deduce the imaginary parts of the first few vertices:

$$\operatorname{Im} X_4 = \operatorname{Im} X_5 < \operatorname{Im} X_6 < \operatorname{Im} X_7 < \operatorname{Im} X_1 = \operatorname{Im} X_2 = 0.$$

Then for the real parts, since $X_1 \dots X_n$ does not intersect itself, we have:

$$\operatorname{Re} X_7 < \operatorname{Re} X_3$$

These inequalities imply that the ray $X_7 X_8$ must intersect either segment $X_2 X_3$ or $X_3 X_4$. This geometrically places X_8 inside the region Ω , so $X_8 \in \Omega$.

We can repeat this process. The position of X_9 relative to X_8 follows the same rotation. The conditions will imply that the ray X_8X_9 must also intersect one of the boundary segments, which in turn implies $X_9 \in \Omega$. For example, for X_{10} , the ray X_9X_{10} will intersect X_3X_4 or X_4X_5 , leading to $X_{10} \in \Omega$.

By induction, we conclude that all subsequent vertices X_k for $k \geq 7$ lie within Ω . \square

Returning to the proof of the main lemma, in the following argument, we will use the techniques from Lemma 16.

Without loss of generality, we can assume $u = 0$. Let Ω be the disk centered at A_0 with radius a_s . According to the lemma's hypothesis, the point H lies on the ray A_vA_{v+1} and $|A_0H| < a_s$, so the point H is inside the disk Ω . If the point H lies on the line segment A_vA_{v+1} , then similar to the proof of Lemma 7, this would contradict the definition of a Minimal Steiner Tree. Therefore, the point H must lie on the extension of the ray A_vA_{v+1} . Let \mathcal{D}_1 be the closed region enclosed by the polygon $A_uA_{u+1} \dots A_vHA_u$, and let $\Gamma_1 = \partial\mathcal{D}_1$. For some $r > s > 0$ to be determined, we establish a complex coordinate system with the origin at A_{v+1} and the positive real axis along the ray $A_{v+1}A_v$. Let

$$X_k = \begin{cases} s + \sum_{i=1}^{6-k} r\omega^i, & 1 \leq k \leq 6 \\ A_{v+k-6}, & 7 \leq k \leq n+6-v \end{cases}$$

where $\omega = e^{\pi i/3}$, and any undefined summation part is taken as 0. Then $\text{Im } X_7 = \text{Im } X_6 = \text{Im } X_1 = 0$. Let \mathcal{D}_2 be the closed region enclosed by the polygon $X_1X_2 \dots X_7$, and let $\Gamma_2 = \partial\mathcal{D}_2$. Note that since $v < 6$, \mathcal{D}_1 is contained in the upper half-plane \mathbb{H} . Therefore, we can choose $r - s, s$ sufficiently large such that $\mathcal{D}_1 \subseteq \mathcal{D}_2$.

We prove by induction on m that $A_{v+m-6} = X_m \in \mathcal{D}_1$ (for $7 \leq m \leq n+6-v$), and the ray $X_{m-1}X_m$ intersects one of the closed segments $X_{m-6}X_{m-5}$ or $X_{m-5}X_{m-4}$.

For the base case $m = 7$, it is clear that $A_{v+1} = X_7 \in \mathcal{D}_1$. Since $\text{Im } X_7 = \text{Im } X_6 = \text{Im } X_1 = 0$, the ray X_6X_7 intersects the closed segment X_1X_2 .

Assume the conclusion holds for $m = k < n+6-v$. Consider the case $m = k+1$:

By the induction hypothesis, $A_{v+k-6} = X_k \in \mathcal{D}_1$. If the segment $X_kX_{k+1} = A_{v+k-6}A_{v+k-5}$ intersects the polygonal chain $X_1 \dots X_k$, then because $X_k \in \mathcal{D}_1 \subseteq \mathcal{D}_2$, the segment X_kX_{k+1} must intersect Γ_1 . This contradicts the fact that $A_0 \dots A_n$ is non-self-intersecting. Therefore, the segment X_kX_{k+1} does not intersect the polygonal chain $X_1 \dots X_k$. Thus, similar to the proof of lemma 16, by the induction hypothesis, since the ray $X_{k-1}X_k$ intersects the closed segment $X_{k-6}X_{k-5}$ or $X_{k-5}X_{k-4}$, the ray X_kX_{k+1} must intersect the closed segment $X_{k-5}X_{k-4}$ or $X_{k-4}X_{k-3}$. Hence, $X_{k+1} \in \mathcal{D}_2$. Since Γ_1 divides \mathcal{D}_2 into two connected components, \mathcal{D}_1 and $(\mathcal{D}_2 - \mathcal{D}_1)$, if $X_{k+1} \in (\mathcal{D}_2 - \mathcal{D}_1)$, then the segment X_kX_{k+1} would intersect Γ_1 , which contradicts the non-self-intersecting property of $A_0 \dots A_n$. Therefore, $X_{k+1} \in \mathcal{D}_1$. By the principle of induction, we conclude that $A_n = X_{n+6-v} \in \mathcal{D}_1$. \square

Full list of type A&B Conditions when $n = 6$ can be found in the following tables.

| B-type Conditions | |
|-------------------|--|
| Condition | Description |
| $C_{0,1,s}^B$ | False |
| $C_{0,2,s}^B$ | $(1 - a_2)/2 \geq 0 \wedge (\sqrt{3}/2 \cdot (1 + a_2) \leq a_s)$ |
| $C_{0,3,s}^B$ | $(2 + a_2 - a_3)/2 \geq 0 \wedge (\sqrt{3}/2 \cdot (a_2 + a_3) \leq a_s)$ |
| $C_{0,4,s}^B$ | $(1 + 2a_2 + a_3 - a_4)/2 \geq 0 \wedge (\sqrt{3}/2 \cdot (-1 + a_3 + a_4) \leq a_s)$ |
| $C_{0,5,s}^B$ | $(-1 + a_2 + 2a_3 + a_4 - a_5)/2 \geq 0 \wedge (\sqrt{3}/2 \cdot (-1 - a_2 + a_4 + a_5) \leq a_s)$ |
| $C_{1,2,s}^B$ | False |
| $C_{1,3,s}^B$ | $(a_2 - a_3)/2 \geq 0 \wedge (\sqrt{3}/2 \cdot (a_2 + a_3) \leq a_s)$ |
| $C_{1,4,s}^B$ | $(2a_2 + a_3 - a_4)/2 \geq 0 \wedge (\sqrt{3}/2 \cdot (a_3 + a_4) \leq a_s)$ |

| | |
|---------------|---|
| $C_{1,5,s}^B$ | $(a_2 + 2a_3 + a_4 - a_5)/2 \geq 0 \wedge (\sqrt{3}/2 \cdot (-a_2 + a_4 + a_5) \leq a_s)$ |
| $C_{2,3,s}^B$ | False |
| $C_{2,4,s}^B$ | $(a_3 - a_4)/2 \geq 0 \wedge (\sqrt{3}/2 \cdot (a_3 + a_4) \leq a_s)$ |
| $C_{2,5,s}^B$ | $(2a_3 + a_4 - a_5)/2 \geq 0 \wedge (\sqrt{3}/2 \cdot (a_4 + a_5) \leq a_s)$ |
| $C_{3,4,s}^B$ | False |
| $C_{3,5,s}^B$ | $(a_4 - a_5)/2 \geq 0 \wedge (\sqrt{3}/2 \cdot (a_4 + a_5) \leq a_s)$ |
| $C_{4,5,s}^B$ | False |

A-type Conditions

| Condition | Description |
|---------------|--|
| $C_{0,1,s}^A$ | $1 \geq a_s$ |
| $C_{0,2,s}^A$ | $1 + a_2 + a_2^2 \geq a_s^2$ |
| $C_{0,3,s}^A$ | $1 + a_2 + a_2^2 - a_3 + a_2 a_3 + a_3^2 \geq a_s^2$ |
| $C_{0,4,s}^A$ | $a_2^2 + a_3^2 + a_2(1 + a_3 - a_4) + a_3(-1 + a_4) + (-1 + a_4)^2 \geq a_s^2$ |
| $C_{0,5,s}^A$ | $1 + a_2^2 + a_3^2 - 2a_4 + a_4^2 + a_2(1 + a_3 - a_4 - 2a_5) + a_3(-1 + a_4 - a_5) - a_5 + a_4 a_5 + a_5^2 \geq a_s^2$ |
| $C_{0,6,s}^A$ | $1 + a_2^2 + a_3^2 - 2a_4 + a_4^2 - a_5 + a_4 a_5 + a_5^2 + a_3(-1 + a_4 - a_5 - 2a_6) + a_2(1 + a_3 - a_4 - 2a_5 - a_6) + a_6 - a_4 a_6 + a_5 a_6 + a_6^2 \geq a_s^2$ |
| $C_{1,2,s}^A$ | $a_2 \geq a_s$ |
| $C_{1,3,s}^A$ | $a_2^2 + a_2 a_3 + a_3^2 \geq a_s^2$ |
| $C_{1,4,s}^A$ | $a_2^2 + a_3^2 + a_2(a_3 - a_4) + a_3 a_4 + a_4^2 \geq a_s^2$ |
| $C_{1,5,s}^A$ | $a_2^2 + a_3^2 + a_4^2 + a_2(a_3 - a_4 - 2a_5) + a_3(a_4 - a_5) + a_4 a_5 + a_5^2 \geq a_s^2$ |
| $C_{1,6,s}^A$ | $a_2^2 + a_3^2 + a_4^2 + a_4 a_5 + a_5^2 + a_3(a_4 - a_5 - 2a_6) + a_2(a_3 - a_4 - 2a_5 - a_6) - a_4 a_6 + a_5 a_6 + a_6^2 \geq a_s^2$ |
| $C_{2,3,s}^A$ | $a_3 \geq a_s$ |
| $C_{2,4,s}^A$ | $a_3^2 + a_3 a_4 + a_4^2 \geq a_s^2$ |
| $C_{2,5,s}^A$ | $a_3^2 + a_4^2 + a_3(a_4 - a_5) + a_4 a_5 + a_5^2 \geq a_s^2$ |
| $C_{2,6,s}^A$ | $a_3^2 + a_4^2 + a_5^2 + a_3(a_4 - a_5 - 2a_6) + a_4(a_5 - a_6) + a_5 a_6 + a_6^2 \geq a_s^2$ |
| $C_{3,4,s}^A$ | $a_4 \geq a_s$ |
| $C_{3,5,s}^A$ | $a_4^2 + a_4 a_5 + a_5^2 \geq a_s^2$ |
| $C_{3,6,s}^A$ | $a_4^2 + a_5^2 + a_4(a_5 - a_6) + a_5 a_6 + a_6^2 \geq a_s^2$ |
| $C_{4,5,s}^A$ | $a_5 \geq a_s$ |
| $C_{4,6,s}^A$ | $a_5^2 + a_5 a_6 + a_6^2 \geq a_s^2$ |
| $C_{5,6,s}^A$ | $a_6 \geq a_s$ |

The proofs of Lemma 7 (necessary properties) and Lemma 8 (sufficient conditions) in this section establish the formal geometric foundation for discovering Trapped Regular Point Lemmas. These predicates constitute one of the two primary paths for systematically constructing new verification functions in our framework.

B.2. Proof of Theorems in Section 4

Theorem 6 (restated). Let $H \subset \mathcal{W}$ be a bounded axis-aligned hyperrectangle and let f be any function in \mathcal{F}_{ver} . A key property is that the global maximum of f over H is attained at one of the vertices. Consequently, if

$$\max_{\mathbf{w} \in \mathcal{V}(H)} f(\mathbf{w}) \leq 0, \quad (4)$$

then $f(\mathbf{w}) \leq 0$ for all $\mathbf{w} \in H$, which implies that the underlying splitting function $g(\mathbf{w}) \leq 0$.

Proof. Since the set of vertices $\mathcal{V}(H)$ is finite, the value $M = \max_{\mathbf{v} \in \mathcal{V}(H)} f(\mathbf{v})$ is well-defined. Consider the sublevel set of f at level M :

$$\mathcal{L}_M = \{\mathbf{w} \in H \mid f(\mathbf{w}) \leq M\}.$$

By the definition of \mathcal{F}_{ver} , \mathcal{L}_M is an orthogonally convex set. By our definition of M , it is clear that all vertices of the hyperrectangle are contained in this set, i.e., $\mathcal{V}(H) \subseteq \mathcal{L}_M$.

To prove that $f(\mathbf{w}_0) \leq M$ for any $\mathbf{w}_0 \in H$, it suffices to show that $H \subseteq \mathcal{L}_M$. We rely on the following geometric lemma:

Lemma 17. *Let $S \subseteq \mathbb{R}^n$ be an orthogonally convex set and $H \subset \mathbb{R}^n$ be a bounded axis-aligned hyperrectangle. If $\mathcal{V}(H) \subseteq S$, then $H \subseteq S$.*

Proof of Lemma. We proceed by induction on the dimension n .

• **Base Case ($n = 1$):** H is an interval $[a, b]$. Since S is orthogonally convex, its intersection with the line containing H is a connected interval. Since the endpoints (vertices) $a, b \in S$, the entire interval $[a, b]$ must be contained in S .

• **Inductive Step:** Assume the statement holds for dimension $n - 1$. Let $H = [a, b] \times H'$, where H' is an $(n - 1)$ -dimensional hyperrectangle. The vertices of H are the union of $\{a\} \times \mathcal{V}(H')$ and $\{b\} \times \mathcal{V}(H')$.

Consider the slice of S at $x_1 = a$, defined as $S_a = \{\mathbf{y} \in \mathbb{R}^{n-1} \mid (a, \mathbf{y}) \in S\}$. Since S is orthogonally convex in \mathbb{R}^n , the slice S_a is orthogonally convex in \mathbb{R}^{n-1} .

Since $\{a\} \times \mathcal{V}(H') \subseteq \mathcal{V}(H) \subseteq S$, it follows that $\mathcal{V}(H') \subseteq S_a$. By the inductive hypothesis, $H' \subseteq S_a$. This implies that the entire face $\{a\} \times H'$ is contained in S . By the same logic, the face $\{b\} \times H'$ is also contained in S .

Now, take any point $\mathbf{w} = (x_1, \mathbf{w}') \in H$. Consider the line segment connecting (a, \mathbf{w}') and (b, \mathbf{w}') . This segment is parallel to the first coordinate axis. Since the endpoints lie in the faces identified above, they are both in S . By the orthogonal convexity of S , the entire segment is in S , implying $\mathbf{w} \in S$.

□

Applying the lemma to \mathcal{L}_M , we conclude that $H \subseteq \mathcal{L}_M$. Therefore, for every $\mathbf{w}_0 \in H$, $f(\mathbf{w}_0) \leq M$. If $M \leq 0$, it immediately follows that $f(\mathbf{w}_0) \leq 0$ everywhere in H . □

Theorem 18. *A series of $F \in \mathcal{F}_{\text{ver}}$ can be derived by establishing one of the following two types of lemmas:*

1. **Trapped Regular Point Lemma:** *A proposition asserting that when the parameters \mathbf{w} satisfy certain linear constraints, an implicit regular point is guaranteed to lie within a specific bounded polygonal region.*
2. **Valid 4-Point Steiner Tree Lemma:** *A proposition asserting that when \mathbf{w} satisfies certain orthogonally convex conditions, a specific 4-point Steiner tree structure is valid.*

Proof. Our objective is to explain how a series of verification functions $F \in \mathcal{F}_{\text{ver}}$ can be derived from these two types of lemmas. Notice that both linear constraints and orthogonally convex conditions restrict the parameter vector \mathbf{w} to an orthogonally convex set Ω .

Consequently, for the first type of lemma, let the trapped regular point be denoted by v_0 . We can consider the set t^* that contains v_0 and its corresponding splitting function:

$$F_\tau(\mathbf{w}, \rho) = \rho \cdot L_{t^*} + L_{S^+} - L_{S^-}.$$

Since v_0 is confined within a certain polygonal region, we can derive an upper bound \tilde{L}_{t^*} for L_{t^*} by estimating the upper bounds of the edges associated with v_0 . Next, we examine whether the function

$$\tilde{F}_\tau(\mathbf{w}, \rho) = \rho \cdot \tilde{L}_{t^*} + L_{S^+} - L_{S^-}$$

satisfies the definition of a verification function, where the underlying splitting function is $F_\tau(\mathbf{w}, \rho)$. If it does, we have successfully obtained a new verification function.

For the second type of lemma, let the vertices of the 4-point Steiner tree be X_1, X_2, X_3, X_4 . We can consider the set S^+ that includes this Steiner tree and its corresponding splitting function:

$$F_\tau(\mathbf{w}, \rho) = \rho \cdot L_{t^*} + L_{S^+} - L_{S^-}.$$

Analogous to the treatment of the first type of lemma, when $\mathbf{w} \in \Omega$, we can derive a new verification function by estimating an upper bound \tilde{L}_{S^+} for L_{S^+} and then checking if

$$\tilde{F}_\tau(\mathbf{w}, \rho) = \rho \cdot L_{t^*} + \tilde{L}_{S^+} - L_{S^-}$$

satisfies the definition of a verification function. By Lemma 15 and the fact that the coordinates of U and V in the statement of the lemma are all affine functions of \mathbf{w} , we conclude that \tilde{L}_{S^+} is convex. Restricting the convex function to the orthogonally convex set Ω yields a verification function. \square

Theorem 9 (restated). Let $\{C_i^A\}_{i=1}^k \subseteq \mathcal{C}^A$ and $\{C_j^B\}_{j=1}^l \subseteq \mathcal{C}^B$ be subsets of conditions. Suppose a linear constraint C on \mathbf{w} satisfies the implication: $C \wedge \left(\bigwedge_{i=1}^k C_i^A\right) \implies \bigvee_{j=1}^l C_j^B$. Then, if \mathbf{w} satisfies C , the regular point A_n is trapped inside the corresponding polygonal region.

Proof. This follows directly from the definitions of Lemma 7 and Lemma 8. \square

Lemma 15 (restated). The length of the (AB) - (CD) type Steiner tree is precisely given by $|UV|$, where U denote the position of point B after segment AB is rotated counterclockwise 60° about point A and V denote the position of point D after segment CD is rotated counterclockwise 60° about point C .

Proof. By construction, points A, U, B are arranged in counterclockwise order and form an equilateral triangle, as are points C, V, D . Consequently, $\triangle ABU$ and $\triangle CVD$ are equilateral triangles.

Recall Definition 10. A key property of the geometry is that the angle between the segments connecting to the non-bridge endpoints at a Steiner point is 120° . Therefore, we note that $\angle ASB = 2\pi/3$. Since $\triangle ABU$ is equilateral, $\angle AUB = \pi/3$. The sum of these opposite angles in the quadrilateral $AUBS$ is $\angle ASB + \angle AUB = 2\pi/3 + \pi/3 = \pi$. This implies that the points A, U, B, S are concyclic.

Since the points are concyclic, the angle $\angle ASU$ subtends the same arc AU as the angle $\angle ABU$. Thus, $\angle ASU = \angle ABU = \pi/3$. From the definition of the Steiner point S , the segments SA, SB , and ST form 120° angles. Specifically, $\angle AST = 2\pi/3$. It follows that $\angle ASU + \angle AST = \pi/3 + 2\pi/3 = \pi$, which proves that the points U, S, T are collinear. By a similar argument for the points C, V, D, T , we can show that V, T, S are also collinear. Combining these results, we conclude that the four points U, S, T, V lie on a single straight line in that order.

Applying Ptolemy's theorem to the cyclic quadrilateral $AUBS$, we have:

$$|AB| \cdot |US| = |AU| \cdot |BS| + |BU| \cdot |AS|.$$

Since $\triangle ABU$ is equilateral, $|AU| = |BU| = |AB|$. Substituting these into the equation and dividing by $|AB|$ yields:

$$|US| = |AS| + |BS|.$$

Similarly, applying Ptolemy's theorem to the cyclic quadrilateral $CVDT$, we obtain:

$$|VT| = |CT| + |DT|.$$

As the points U, S, T, V are collinear, the length of the segment $|UV|$ is the sum of the lengths of the constituent segments:

$$|UV| = |US| + |ST| + |TV| = (|AS| + |BS|) + |ST| + (|CT| + |DT|).$$

This sum is precisely the total length of the edges in the (AB) - (CD) type Steiner tree. \square

This section proves two cornerstone components of our theoretical framework:

1. **Theorem 6 (Vertex-Maximization Property)** is the foundation of our entire verification strategy. It fundamentally addresses the challenge of computational tractability by reducing the verification problem over a continuous parameter domain to a check on its discrete vertices¹
2. **Pathways for Constructing New Verification Functions:** The efficacy of Theorem 6 relies on a sufficiently rich set of verification functions, \mathcal{F}_{ver} . Our framework systematically augments this set by establishing two types of lemmas:
 - **Trapped Regular Point Lemma:** Theorem 9 formally establishes this pathway. It leverages the A/B predicates from Section B.1 to transform the search for such lemmas into a formal logical deduction task.
 - **Valid 4-Point Steiner Tree Lemma:** This second pathway is designed to handle more complex 4-point splits. Based on Theorem 14, it operates by identifying additional geometric constraints that ensure the corresponding complex splitting function satisfies the shape constraints required by Theorem 6.

B.3. Proof of Convexity for Splitting Functions

In this section, we provide the proof that for any split where the component S^+ connects a set of terminals of size at most 3 (i.e., $|S^+| \leq 3$), the resulting splitting function $F(\mathbf{w}, \rho)$ is a convex function of the geometric parameters \mathbf{w} .

Recall the definition of the splitting function:

$$F(\mathbf{w}, \rho) = \rho \cdot L_{t^*}(\mathbf{w}) + L_{S^+}(\mathbf{w}) - L_{S^-}(\mathbf{w}).$$

We analyze the convexity of each term individually. Since we directly use edge lengths as parameters, the coordinates of points in the local substructure are affine functions of the parameter vector \mathbf{w} .

B.3.1. LINEARITY OF L_{S^-}

The term L_{S^-} represents the sum of the lengths of the edges removed from the original Steiner tree. In our local parameterization, the edge lengths of the initial tree S are directly used as the parameters (or linear combinations thereof). Consequently, $L_{S^-}(\mathbf{w})$ is an affine function of \mathbf{w} and therefore $-L_{S^-}(\mathbf{w})$ preserves convexity.

B.3.2. CONVEXITY OF L_{t^*}

The term L_{t^*} represents the length of the connector graph t^* , which consists of edges connecting specific pairs of points from V . Let $\mathbf{u}(\mathbf{w})$ and $\mathbf{v}(\mathbf{w})$ be the coordinates of two such points. The Euclidean distance between them is:

$$d(\mathbf{u}, \mathbf{v}) = \|\mathbf{u}(\mathbf{w}) - \mathbf{v}(\mathbf{w})\|_2.$$

The Euclidean norm $\|\cdot\|_2$ is a convex function and $\mathbf{u}(\mathbf{w}) - \mathbf{v}(\mathbf{w})$ is affine in \mathbf{w} . The composition of a convex function with an affine mapping is convex. Thus, the distance between any pair of points is convex in \mathbf{w} . Since L_{t^*} is a sum of such distances (with $\rho \geq 0$), $\rho \cdot L_{t^*}(\mathbf{w})$ is convex.

B.3.3. CONVEXITY OF L_{S^+} FOR $|S^+| \leq 3$

The term L_{S^+} denotes the length of the Steiner Minimal Tree for a subset of boundary points $V' \subset \mathbb{R}^2$. We consider the cases where $|V'| \leq 3$.

Case 1: $|V'| \leq 2$. If $|V'| = 2$, L_{S^+} is simply the Euclidean distance between the two points. If $|V'| < 2$, the length is 0. In both cases, the convexity follows the same logic as Section B.3.2.

Case 2: $|V'| = 3$. Let $V' = \{A, B, C\}$. The length of the Steiner Minimal Tree is obtained by introducing at most one Steiner point q . The length function is defined by the minimization problem:

$$L_{S^+}(\mathbf{w}) = \inf_{\mathbf{q} \in \mathbb{R}^2} (\|A(\mathbf{w}) - \mathbf{q}\|_2 + \|B(\mathbf{w}) - \mathbf{q}\|_2 + \|C(\mathbf{w}) - \mathbf{q}\|_2).$$

¹The algorithm implementing this vertex-checking strategy is provided in Appendix D.1.

Let $g(\mathbf{w}, \mathbf{q}) = \|A(\mathbf{w}) - \mathbf{q}\|_2 + \|B(\mathbf{w}) - \mathbf{q}\|_2 + \|C(\mathbf{w}) - \mathbf{q}\|_2$. Note that the term $\|A(\mathbf{w}) - \mathbf{q}\|_2$ is the Euclidean norm of an affine function of the joint vector (\mathbf{w}, \mathbf{q}) . Therefore, it is jointly convex in (\mathbf{w}, \mathbf{q}) . Since the sum of convex functions is convex, $g(\mathbf{w}, \mathbf{q})$ is jointly convex in \mathbf{w} and \mathbf{q} .

We invoke the standard result from convex analysis: *if $g(x, y)$ is jointly convex in (x, y) and C is a convex set, then the function $h(x) = \inf_{y \in C} g(x, y)$ is convex in x .* Applying this to our case, $L_{S^+}(\mathbf{w}) = \inf_{\mathbf{q}} g(\mathbf{w}, \mathbf{q})$ is a convex function of \mathbf{w} .

B.3.4. CONCLUSION

The splitting function $F(\mathbf{w}, \rho)$ is the sum of a convex term (ρL_{t^*}) , a convex term (L_{S^+}) , and an affine term $(-L_{S^-})$. Since the sum of convex functions is convex, $F(\mathbf{w}, \rho)$ is convex with respect to \mathbf{w} .

This section proves the convexity of a class of basic splitting functions. As these functions inherently satisfy the constraints required by Theorem 6, they serve as the initial members of our verification set \mathcal{F}_{ver} . This set is then subsequently augmented by new functions discovered via the two pathways outlined in the previous subsection.

B.4. Theoretical Foundation for the Monotonicity Check

In the Feasibility Verification Algorithm, we encounter unbounded hyperrectangles where some edge length parameters extend to $+\infty$. To handle these regions without evaluating limits explicitly, we verify that the splitting function $F(\mathbf{w}, \rho)$ is monotonically non-increasing with respect to the unbounded parameter. This section establishes the geometric foundations and the algorithmic implementation of this check.

We first describe the verification procedure designed for the splits where $|S^+| \leq 3$ that do not involve implicit regular points.

B.4.1. GEOMETRIC FOUNDATIONS

Let x be the parameter representing the length of a specific edge e in the tree topology. We first establish upper bounds on the partial derivatives of the length components with respect to x .

Lemma 19 (Derivative of Path Length). *Let t^* be a graph connecting points in V , and let L_{t^*} be its total length. Then:*

$$\frac{\partial L_{t^*}}{\partial x} \leq \sum_{(u,v) \in t^*} \mathbb{I}(e \in \text{path}(u, v)),$$

where $\mathbb{I}(\cdot)$ is the indicator function, and $\text{path}(u, v)$ denotes the unique path between u and v in the full tree structure.

Proof. Let (u, v) be an edge in t^* . Its length is the Euclidean distance $\|u(\mathbf{w}) - v(\mathbf{w})\|$. If the edge e (associated with parameter x) does not lie on the path between u and v in the underlying tree, then u and v belong to the same rigid component with respect to e . Changing x translates both points identically, so $\|u - v\|$ is constant, and the derivative is 0.

If e lies on the path between u and v , increasing x translates one endpoint (say v) relative to the other (u) by a vector \mathbf{d} with $\|\mathbf{d}\| = 1$ (the unit direction of edge e). The derivative is:

$$\frac{\partial \|u - v\|}{\partial x} = \langle \nabla_v \|u - v\|, \mathbf{d} \rangle = \left\langle \frac{v - u}{\|v - u\|}, \mathbf{d} \right\rangle = \cos \theta,$$

where θ is the angle between the chord uv and the edge e . Since $\cos \theta \leq 1$, the derivative is bounded by 1. Summing over all edges in t^* yields the result. \square

Lemma 20 (Derivative of SMT Length). *Let S^+ be the Steiner Minimal Tree for a set of terminals V' , with $|V'| \leq 3$. Then:*

$$\frac{\partial L_{S^+}}{\partial x} \leq 1.$$

Proof. If $|V'| \leq 2$, L_{S^+} is a single Euclidean distance (or 0), and the result follows from Lemma 19.

Consider the case $|V'| = 3$, say $V' = \{A, B, C\}$. The SMT consists of a Steiner point q connecting to A, B, C . The length is $L = \|A - q\| + \|B - q\| + \|C - q\|$. By the Envelope Theorem, the derivative of the optimal value function with respect

to a parameter is equal to the partial derivative of the objective function evaluated at the optimum. Thus, we do not need to consider the change in the optimal position of q . If edge e separates the terminals (e.g., separating A from $\{B, C\}$), increasing x translates A relative to the rest of the system by a unit vector \mathbf{d} . The derivative is:

$$\frac{\partial L}{\partial x} = \frac{\partial \|A-q\|}{\partial x} = \left\langle \frac{A-q}{\|A-q\|}, \mathbf{d} \right\rangle = \cos \theta \leq 1.$$

If e does not separate the terminals, they move as a rigid body, and the derivative is 0. In all cases, the upper bound is 1. \square

B.4.2. SPECIAL ANALYSIS ON THE MONOTONICITY OF f

We extend Lemma 20 to S^+ connecting a set of terminals whose size is larger than 3.

Lemma 21 (Derivative of SMT Length with respect to f). *Let S^+ be the Steiner Minimal Tree for a set of terminals V' . Then:*

$$\frac{\partial L_{S^+}}{\partial f} \leq 1.$$

Proof. If $Q \notin V'$, then clearly $\frac{\partial L_{S^+}}{\partial f} = 0$. Now we focus on the case where $Q \in V'$. Fix the values of all variables except f . Let $h(x)$ denote the value of L_{S^+} when $f = x$. We then prove that for any $0 \leq x_1 < x_2$, $h(x_2) - h(x_1) \leq x_2 - x_1$.

Let Q_1 and Q_2 denote the positions of point Q when $f = x_1$ and $f = x_2$, respectively. Let V'' be the set of vertices in V' excluding Q . Since $SMT(V'' \cup \{Q_1\})$ together with the edge Q_1Q_2 forms a Steiner tree for $V'' \cup \{Q_2\}$, we have $L_S(V'' \cup \{Q_2\}) \leq L_S(V'' \cup \{Q_1\}) + |Q_1Q_2|$, which by definition implies $h(x_2) - h(x_1) \leq x_2 - x_1$. \square

Based on Lemma 21, when verifying monotonicity with respect to variable f , we can apply the monotonicity check procedure to the splits generated by the LLM using the 4-Point Steiner Tree Lemmas. This forms a key foundation for the reduction strategy for unbounded f in Appendix E.2.

The vertex-checking strategy of Theorem 6 is not directly applicable to unbounded parameter regions. To address this case, we must first verify the function's monotonicity along any unbounded dimensions, thereby reducing the problem to one on a bounded domain. The lemmas presented in this section (Lemmas 19, 20, and 21) provide the necessary theoretical guarantees for this critical monotonicity check.

B.5. Correctness Proof for Algorithm 2

We assume $\rho \leq 1$, which is valid for the Steiner ratio problem. Recall the derivative of the splitting function:

$$\frac{\partial F}{\partial x} = \rho \frac{\partial L_{t^*}}{\partial x} + \frac{\partial L_{S^+}}{\partial x} - \frac{\partial L_{S^-}}{\partial x}.$$

We analyze the bounds using the variables computed in Algorithm 2:

- Since S^- is a fixed tree topology and x is the length of edge e , $\frac{\partial L_{S^-}}{\partial x} = \delta_{S^-}$.
- By Lemma 19, $\frac{\partial L_{t^*}}{\partial x} \leq N_{t^*}$.
- By Lemma 20, $\frac{\partial L_{S^+}}{\partial x} \leq \delta_{S^+}$.

Substituting these into the derivative:

$$\frac{\partial F}{\partial x} \leq \rho \cdot N_{t^*} + \delta_{S^+} - \delta_{S^-} \leq N_{t^*} + \delta_{S^+} - \delta_{S^-}. \quad (5)$$

The algorithm returns **True** only if $N_{t^*} + \delta_{S^+} \leq 1$ and $\delta_{S^-} = 1$ (or if all terms are 0).

1. If all terms are 0, the derivative is 0.
2. Otherwise, we have $\delta_{S^-} = 1$. Since $N_{t^*} + \delta_{S^+} \leq 1$, inequality 5 becomes $\frac{\partial F}{\partial x} \leq N_{t^*} + \delta_{S^+} - 1 \leq 0$

In all accepted cases, $\frac{\partial F}{\partial x} \leq 0$. Thus, Algorithm 2 provides a rigorous sufficient condition for monotonicity.

By combining the theoretical foundations from Section B.4 with the proof of correctness in this section, we establish the formal rigor of our entire verification pipeline. This ensures its reliability in handling both bounded and unbounded parameter regions, thus providing comprehensive support for the application of Theorem 6.

C. Proofs of LLM-Generated Lemmas

In this section, we present the formal proofs for the geometric lemmas generated by the LLM agent during the iterative process. As discussed in Section E.2, the LLM proposes these lemmas based on the representative regime where D is a **regular point** and the parameter f is fixed at its boundary value $f = d$.

| Results of Each Step | | | |
|----------------------|---------------|-----------------------|---|
| Step | Steiner Ratio | Proposed Lemma Type | Description |
| 1 | 0.8282 | / | / |
| 2 | 0.8500 | Trapped Regular Point | $C_{0,4,2}^B$ |
| 3 | 0.8502 | Trapped Regular Point | $C_{2,4,3}^A, C_{0,4,3}^B$ |
| 4 | 0.8519 | 4-Point Steiner Tree | $(DQ)-(RA)$ |
| 5 | 0.8536 | 4-Point Steiner Tree | $(AD)-(QR)$ |
| 6 | 0.8540 | Trapped Regular Point | $C_{2,4,3}^B$ |
| 7 | 0.8542 | 4-Point Steiner Tree | $(BD)-(QR)$ |
| 8 | 0.8558 | 4-Point Steiner Tree | $(AD)-(QR)'$ |
| 9 | 0.8559 | Trapped Regular Point | $C_{0,5,5}^A, C_{1,5,5}^A, C_{0,5,5}^B$ |

Table 2. Results of Each Step

To apply these lemmas to the global verification problem (spanning all four cases defined in Section E.2), we adhere to the following transplantation policies:

- 1. Trapped Regular Point Lemmas (Implicit E):** These lemmas rely exclusively on the local geometry of the chain starting at A . The validity of the implication $C \implies \text{Trapped}(E)$ is independent of the topology of D or the value of f . Therefore, these lemmas are **universally transplanted** to all four cases.
- 2. 4-Point Steiner Tree Lemmas:** These lemmas (e.g., verifying the existence of $(AD)-(QR)$ trees) were derived and symbolically verified under the strict assumption $f = d$.
 - Cases 2 & 4 ($f \geq d$):** As per our reduction strategy, the verification functions for the unbounded domain $f \in (d, +\infty)$ are mapped to the boundary $f = d$. Thus, these lemmas are **valid and applied**.
 - Cases 1 & 3 ($f \leq d$):** In these regimes, the geometric validity of a 4-point topology depends on the specific value of $f \in [0, d]$. Since the symbolic verification was not performed for variable f , we adopt a conservative policy: we **exclude** these high-complexity 4-point tree lemmas in these cases, relying instead on the baseline splits and trapped point lemmas.

Edge lengths follow the notation in Figure 11. For example, $|AY| = \sqrt{1 + s + s^2}$ and $|AZ| = \sqrt{1 + s + s^2 - c + cs + c^2}$.

Step 1

Lemma 22 (Step 1, Side A). *If $c < 1$, then there exists a regular point E such that $|AE| \leq \max\{|AY|, |AZ|\}$.*

Lemma 23 (Step 1, Side D). *If $f < d$, then there exists a regular point F such that $|DF| \leq \max\{|DZ|, |DQ|\}$.*

Note that these 2 lemmas are the same as Corollary 33 and Corollary 34, respectively, when D is a regular point. We restated them here for a clearer step-by-step proof.

Step 2

Lemma 24 (Step 2). *If $e < 1 - c + 2/\sqrt{3} \cdot s$ and $c + e > 1$, then there exists a regular point E such that $|AE| \leq \max\{1, |AY|, |AZ|, |AR|, \sqrt{3}/2 \cdot (c + e - 1)\}$.*

Proof. If R is a regular point, the statement is proved. We now assume R is a Steiner point. For a Minimal Steiner Tree, this implies the existence of a subsequent edge emanating from R in the clockwise direction. Let H be the foot of the perpendicular from point A to the line containing this edge. Note that $C_{0,4,2}^B$ is $1 + 2s + c - e > 0$ and $\sqrt{3}/2 \cdot (-1 + c + e) \leq s$. We show that $C_{0,4,2}^B$ holds under the lemma conditions.

First, from $e < 1 - c + 2/\sqrt{3} \cdot s$, we have $1 + 2s + c - e > 1 + 2(\sqrt{3}/2 \cdot (-1 + c + e)) + c - e = 1 - \sqrt{3} + (1 + \sqrt{3})c + (\sqrt{3} - 1)e$. Note that if $c < 1$, then by Lemma 22 we already have $|AE| \leq \max\{|AY|, |AZ|\}$, so we only need to consider the case $c \geq 1$. Thus $1 + 2s + c - e > 1 - \sqrt{3} + (1 + \sqrt{3})c + (\sqrt{3} - 1)e \geq 2 + (\sqrt{3} - 1)e > 0$. Second, we have $\sqrt{3}/2 \cdot (-1 + c + e) < \sqrt{3}/2 \cdot (2/\sqrt{3} \cdot s) = s$. Thus, $C_{0,4,2}^B$ holds. Then by Theorem 9, there exists a regular point E trapped inside the polygonal region $AXYZRH$. Since $|AH| = \sqrt{3}/2 \cdot (c + e - 1)$ by simple calculation, we have $|AE| \leq \max\{1, |AY|, |AZ|, |AR|, \sqrt{3}/2 \cdot (c + e - 1)\}$. \square

Step 3

Lemma 25 (Step 3). *If $e < 1 + (2/\sqrt{3} - 1) \cdot c$ and $c + e > 1$, then there exists a regular point E such that $|AE| \leq \max\{1, |AY|, |AZ|, |AR|, \sqrt{3}/2 \cdot (c + e - 1)\}$.*

Proof. If R is a regular point, the statement is proved. We now assume R is a Steiner point. For a Minimal Steiner Tree, this implies the existence of a subsequent edge emanating from R in the clockwise direction. Let H be the foot of the perpendicular from point A to the line containing this edge. Note that $C_{0,4,3}^B$ is $1 + 2s + c - e > 0$ and $\sqrt{3}/2 \cdot (-1 + c + e) \leq c$. We show that $C_{0,4,3}^B$ holds under the lemma conditions.

The first part is same as Lemma 24. For the second part, from $e < 1 + (2/\sqrt{3} - 1) \cdot c$, we have $\sqrt{3}/2 \cdot (-1 + c + e) < \sqrt{3}/2 \cdot ((2/\sqrt{3} - 1) \cdot c + c) = c$. Thus, $C_{0,4,3}^B$ holds. Then by Theorem 9, there exists a regular point E trapped inside the polygonal region $AXYZRH$, so we can conclude the proof same as Lemma 24. \square

Step 4

Lemma 26 (Step 4). *The region defined by the system of inequalities \mathcal{S} below is an orthogonally convex set. Furthermore, for any w in this region, the (RA)-(DQ) type Steiner tree is valid.*

$$\mathcal{S} : \begin{cases} I_1 : e + c \geq 1 \\ I_2 : e \leq s + c + d + 2 \\ I_3 : e \geq 2 - c - d + s \\ I_4 : e \leq 3s \\ I_5 : (2 + c^2 + 3d + 2s + 3cs + 3ds + 2s^2) - (2 + c + 3d + s)e \geq 0 \\ I_6 : 2(\vec{RD} \cdot \vec{AQ}) + |\vec{RD}| |\vec{AQ}| \geq 0 \\ I_7 : 2(\vec{RV} \cdot \vec{RA}) + |\vec{RV}| |\vec{RA}| \geq 0 \\ I_8 : 2(\vec{AV} \cdot \vec{AR}) + |\vec{AV}| |\vec{AR}| \geq 0 \end{cases}$$

Proof. We perform the verification in two parts: first demonstrating that these conditions imply the geometric existence of the tree, and second proving that the defined region is orthogonally convex.

We employ **Cylindrical Algebraic Decomposition (CAD)** to rigorously verify all the following inequalities.

PART 1: GEOMETRIC VALIDITY

We verify the sufficient conditions from Theorem 14. To enable algebraic verification, all angular conditions $\theta \leq 120^\circ$ are transformed into the equivalent scalar product inequality:

$$2(\vec{u} \cdot \vec{v}) + |\vec{u}| |\vec{v}| \geq 0.$$

1. Convexity of Quadrilateral $RADQ$:

- $\vec{RA} \times \vec{AD} \leq 0$, $\vec{AD} \times \vec{DQ} \leq 0$, and $\vec{DQ} \times \vec{QR} \leq 0$: Verified unconditionally.
- $\vec{QR} \times \vec{RA} \leq 0$: Verified to hold when $c + e \geq 1$, which is explicitly enforced by inequality I_1 .

2. Simpson Point Angles:

- $\angle UDQ \leq 120^\circ$: The condition I_2 implies that $\vec{DU} \cdot \vec{DQ} \geq 0$ (i.e., the angle is $\leq 90^\circ$), which sufficiently implies $\leq 120^\circ$.
- $\angle UQD \leq 120^\circ$: The condition I_3 implies that $\vec{QU} \cdot \vec{QD} \geq 0$ (i.e., the angle is $\leq 90^\circ$), which sufficiently implies $\leq 120^\circ$.
- $\angle VRA \leq 120^\circ$: This is the direct geometric interpretation of inequality I_7 .
- $\angle VAR \leq 120^\circ$: This is the direct geometric interpretation of inequality I_8 .

3. Intersection Angle:

- The condition that the angle between diagonals RD and AQ is $\leq 120^\circ$ corresponds directly to inequality I_6 .

PART 2: ORTHOGONAL CONVEXITY CHECK

We verify that each defining inequality in \mathcal{S} is monotonic with respect to the coordinate axes within the feasible region.

Linear Inequalities (I_1, I_2, I_3, I_4): These are linear combinations of variables. Linear functions are unconditionally monotonic, thus defining orthogonally convex half-spaces.

Inequality I_5 : Let $g_5(\mathbf{w})$ be the LHS of I_5 .

- Variables d, e : The function g_5 is linear with respect to d and e , ensuring monotonicity.
- Variable s : We compute $\frac{\partial g_5}{\partial s}$. Symbolic verification confirms $\frac{\partial g_5}{\partial s} \geq 0$ whenever $e \leq s + c + d + 2$. This condition is ensured by I_2 .
- Variable c : We compute $\frac{\partial g_5}{\partial c}$. Symbolic verification confirms $\frac{\partial g_5}{\partial c} \geq 0$ whenever $e \leq 3s$. This condition is ensured by I_4 .

Inequality I_6 : Let $G(\mathbf{w}) = \frac{\vec{RD} \cdot \vec{AQ}}{|\vec{RD}| |\vec{AQ}|}$ be the cosine of the angle between the diagonals. The condition is equivalent to $G(\mathbf{w}) \geq -1/2$. We analyze the connectivity of the feasible region along lines parallel to each coordinate axis.

- **Variables c and e :** Symbolic differentiation confirms that $\frac{\partial G}{\partial c} \leq 0$ and $\frac{\partial G}{\partial e} \geq 0$ unconditionally. Thus, G is monotonic along the c and e axes, ensuring the feasible region is a connected interval (orthogonally convex) in these directions.
- **Variable s :** The symbolic engine indicates that the sign of $\frac{\partial G}{\partial s}$ depends on c :

$$\operatorname{sgn} \left(\frac{\partial G}{\partial s} \right) = \begin{cases} \geq 0 & \text{if } c \geq 1 \\ \leq 0 & \text{if } c \leq 1 \end{cases}$$

To prove orthogonal convexity, consider any line L parallel to the s -axis. On such a line, the parameters c, d, e are fixed constants. Consequently, the sign of the derivative with respect to s is constant along the entire line L . Thus, G restricted to L is monotonic, and the sublevel set $\{s \in L \mid G(\dots, s, \dots) \geq -1/2\}$ is a connected interval.

- **Variable d :** Similarly, the behavior depends on c :

- If $c \geq 1$: Symbolic verification shows $\frac{\partial G}{\partial d} \geq 0$. G is monotonic, so the intersection is an interval.
- If $c < 1$: Symbolic verification confirms that $G(\mathbf{w}) \geq -1/2$ is satisfied for all admissible d . The intersection is the entire domain $[0, +\infty)$, which is a connected interval.

In all cases, the intersection with lines parallel to the d -axis is connected.

Inequality I_7 : Let $G(\mathbf{w}) = \frac{\vec{RV} \cdot \vec{RA}}{|\vec{RV}| |\vec{RA}|}$. The condition is equivalent to $G(\mathbf{w}) \geq -1/2$. We analyze the properties under the assumption that $c + e \geq 1$ (Inequality I_1).

- **Variables** s, d, e : Symbolic differentiation confirms that within the region $c + e \geq 1$:

$$\frac{\partial G}{\partial s} \leq 0, \quad \frac{\partial G}{\partial d} \leq 0, \quad \frac{\partial G}{\partial e} \geq 0.$$

Since the function is monotonic with respect to each of these variables individually, the feasible region is orthogonally convex along these axes.

- **Variable** c : The behavior depends on the fixed values of s and e :

- If $e \leq s + 1$: Symbolic verification shows $\frac{\partial G}{\partial c} \geq 0$. The function is monotonic, so the valid set for c is a connected interval.
- If $e > s + 1$: Symbolic verification confirms that $G(\mathbf{w}) \geq -1/2$ holds unconditionally for all valid c . The valid set is the entire domain, which is a connected interval.

Thus, for any fixed s, d, e , the set of valid c values is connected.

Inequality I_8 : Let $\mathbf{u} = \vec{AV}$ and $\mathbf{v} = \vec{AR}$. The condition is equivalent to the angle inequality $\angle(\mathbf{u}, \mathbf{v}) \leq 120^\circ$. We verify this by analyzing the inclination angles ϕ and ψ of \mathbf{u} and \mathbf{v} respectively.

Geometric Constraint: We explicitly verify that under the given constraints, the y -components of \vec{AV} and \vec{AR} are always non-positive. Consequently, the vectors lie in the lower half-plane, and their inclination angles ϕ, ψ are well-defined and restricted to the interval $[-180^\circ, 0]$. This ensures no discontinuity in the angle definition.

The condition is thus equivalent to:

$$-120^\circ \leq \Phi(\mathbf{w}) \leq 120^\circ, \quad \text{where } \Phi(\mathbf{w}) = \phi(\mathbf{w}) - \psi(\mathbf{w}).$$

To prove orthogonal convexity, it suffices to show that for any axis-parallel line, Φ is monotonic (or the condition is unconditionally true). We utilize the derivative formula for the inclination angle ϕ of a vector \mathbf{u} :

$$\frac{\partial \phi}{\partial x} = \frac{\det(\mathbf{u}, \partial_x \mathbf{u})}{|\mathbf{u}|^2}.$$

- **Variable** c : The behavior depends on the parameters e and s :

- If $e \geq s + 1$: Symbolic verification shows $\frac{\partial \phi}{\partial c} \leq 0$ and $\frac{\partial \psi}{\partial c} \geq 0$. Thus, $\frac{\partial \Phi}{\partial c} \leq 0$. The difference is monotonic, so the valid set is an interval.
- If $e < s + 1$: Symbolic verification confirms that the angle condition holds unconditionally. The valid set is the entire domain.

Since the condition $e \geq s + 1$ is independent of c , any line parallel to the c -axis falls entirely into one of these two cases.

- **Variable** s : We rely on Inequality I_1 ($c + e \geq 1$). Symbolic verification confirms that when $c + e \geq 1$:

$$\frac{\partial \phi}{\partial s} \leq 0, \quad \frac{\partial \psi}{\partial s} \geq 0 \implies \frac{\partial \Phi}{\partial s} \leq 0.$$

Thus, Φ is monotonic along the s -axis.

- **Variable** d : Symbolic verification shows $\frac{\partial \psi}{\partial d} = 0$. The sign of $\frac{\partial \phi}{\partial d}$ depends on the sum $c + s$:

$$\operatorname{sgn} \left(\frac{\partial \Phi}{\partial d} \right) = \operatorname{sgn} \left(\frac{\partial \phi}{\partial d} \right) = \begin{cases} \geq 0 & \text{if } c + s \geq 1 \\ \leq 0 & \text{if } c + s \leq 1 \end{cases}$$

Consider any line parallel to the d -axis. Along this line, c and s are fixed constants. Thus, the derivative's sign is constant, implying Φ is monotonic along that line.

- **Variable** e : Symbolic verification shows $\frac{\partial \phi}{\partial e} = 0$ and $\frac{\partial \psi}{\partial e} \leq 0$. Thus, $\frac{\partial \Phi}{\partial e} \geq 0$. The function is monotonic along the e -axis.

Final Conclusion: We have demonstrated that for every inequality I_1 through I_8 , the defining constraints satisfy the coordinate-wise monotonicity property (either directly or via case-based logic where the case condition is constant along the axis). Therefore, the intersection of these regions is an orthogonally convex set. \square

Step 5

Lemma 27 (Step 5). *If $c \geq 1$ and $e \geq 1$, then (AD)-(QR) type Steiner tree is valid.*

Proof. We verify the sufficient conditions for the existence of the (AD)-(QR) topology (Theorem 14) using the symbolic computation engine *Mathematica*. To enable algebraic verification, all angular conditions $\theta \leq 120^\circ$ are transformed into the equivalent scalar product inequality:

$$2(\vec{u} \cdot \vec{v}) + |\vec{u}||\vec{v}| \geq 0.$$

We employ **Cylindrical Algebraic Decomposition (CAD)** to rigorously verify that the following inequalities hold under the assumptions $c \geq 1$ and $e \geq 1$:

1. Convexity of Quadrilateral ADQR (via cross products):

- $\vec{AD} \times \vec{DQ} \leq 0$ and $\vec{DQ} \times \vec{QR} \leq 0$: Verified (Unconditional).
- $\vec{QR} \times \vec{RA} \leq 0$: Verified (Requires $c \geq 1$).
- $\vec{RA} \times \vec{AD} \leq 0$: Verified (Unconditional).

2. Simpson Point Angles (via transformed inequality):

- $\angle UQR \leq 120^\circ$, $\angle VAD \leq 120^\circ$, $\angle VDA \leq 120^\circ$: Verified (Unconditional).
- $\angle URQ \leq 120^\circ$: Verified (Requires $e \geq 1$).

3. Intersection Angle (via transformed inequality):

- Angle between diagonals AQ and $DR \leq 120^\circ$: Verified (Requires $c \geq 1$).

4. Orthogonal Convexity: The validity region is defined by the intersection of linear inequalities. Since these are intersections of convex sets, the resulting domain is convex. \square

Step 6

Lemma 28 (Step 6). *If $e < (2/\sqrt{3} - 1) \cdot c$, then there exists a regular point E such that $|AE| \leq \max\{|AY|, |AZ|, |AR|\}$, and $|DE| \leq \max\{|DY|, |DZ|, |DR|, \sqrt{3/4 \cdot (c+e)^2 + 3/2 \cdot (c+e)d + d^2}\}$.*

Proof. We first analyze point R under condition $C_{2,4,3}^B$. If R is a regular point, the statement is proved. We therefore proceed by considering the case where R is a Steiner point. For a Minimal Steiner Tree, this implies the existence of a subsequent edge emanating from R in the clockwise direction. Let H be the foot of the perpendicular from point Y to the line containing this edge. It follows that a trapped regular point, which we denote by E , exists within the polygonal region $YZRH$. The distance $|AM|$ is therefore bounded by:

$$|AE| \leq \max\{|AY|, |AZ|, |AR|, |AH|\}$$

It is clear that $|AH| \leq |AR|$, a consequence of the geometric construction. The reasoning is that the projections of the segments YX and XA onto the line RH are co-directional with the vector \vec{RH} .

Similarly, for the distance between D and the trapped point E , we have the inequality:

$$|DE| \leq \max\{|DY|, |DZ|, |DR|, |DH|\}$$

A calculation yields $|YH| = \frac{\sqrt{3}}{2}(c + e)$. Given that $\angle DYH = 150^\circ$, an application of the Law of Cosines to $\triangle DYH$ gives:

$$\begin{aligned} |DH|^2 &= |DY|^2 + |YH|^2 - 2|DY||YH|\cos(150^\circ) \\ &= |DY|^2 + |YH|^2 + \sqrt{3}|DY||YH| \\ &= d^2 + \frac{3}{2}d(c + e) + \frac{3}{4}(c + e)^2. \end{aligned}$$

□

Step 7

Lemma 29 (Step 7). *If $d \geq b$, then (BD) - (QR) type Steiner tree is valid.*

Proof. We verify the sufficient conditions for the existence of the (BD) - (QR) topology (Theorem 14) using the symbolic computation engine **Mathematica**. As in the previous proof, all angular conditions $\theta \leq 120^\circ$ are transformed into the equivalent scalar product inequality:

$$2(\vec{u} \cdot \vec{v}) + |\vec{u}||\vec{v}| \geq 0.$$

We employ **Cylindrical Algebraic Decomposition (CAD)** to rigorously verify that the following inequalities hold under the assumption $d \geq b$:

1. Convexity of Quadrilateral $BDQR$ (via cross products):

- $\vec{BD} \times \vec{DQ} \leq 0$, $\vec{DQ} \times \vec{QR} \leq 0$, $\vec{QR} \times \vec{RB} \leq 0$, and $\vec{RB} \times \vec{BD} \leq 0$: All verified to hold unconditionally within the geometric domain.

2. Simpson Point Angles (via transformed inequality):

- $\angle U R Q \leq 120^\circ$ and $\angle V B D \leq 120^\circ$: Verified (Unconditional).
- $\angle U Q R \leq 120^\circ$: Verified (Requires $d \geq b$).
- $\angle V D B \leq 120^\circ$: Verified (Requires $d \geq b$).

3. Intersection Angle (via transformed inequality):

- Angle between diagonals BQ and $DR \leq 120^\circ$: Verified (Unconditional).

4. Orthogonal Convexity: The validity region is defined by the linear inequality $d \geq b$, which is automatically convex. □

Step 8

Lemma 30 (Step 8). *The region defined by the system of inequalities \mathcal{S} below is an orthogonally convex set. Furthermore, for any w in this region, the (AD) - (QR) type Steiner tree is valid.*

$$\mathcal{S} : \begin{cases} I_1 : d(c + e - 1) + e(s + c) \geq 0 \\ I_2 : e \geq \frac{1}{2} \left(\sqrt{(c + s + 2d)^2 + 4d} - (c + s + 2d) \right) \\ I_3 : -(1 + s/2 - c/2 + d/2)(c/2 + e + d) + \frac{3}{4}c(s + c + d) \geq 0 \\ I_4 : s + e \geq 1 \\ I_5 : c \leq 1 + d + s/2 + e/2 \end{cases}$$

Proof. We perform the verification in two parts: first demonstrating that these conditions imply the geometric existence of the tree, and second proving that the defined region is orthogonally convex.

We employ **Cylindrical Algebraic Decomposition (CAD)** to rigorously verify all the following inequalities.

PART 1: GEOMETRIC VALIDITY

We verify the sufficient conditions from Theorem 14.

1. Convexity of Quadrilateral $ADQR$:

- The convexity conditions at vertices A, D, Q are verified to hold unconditionally.
- At vertex R , the condition $\vec{QR} \times \vec{RA} \leq 0$ is algebraically equivalent to inequality I_1 .

2. Simpson Point Angles:

- $\angle UQR \leq 120^\circ, \angle VAD \leq 120^\circ$, and $\angle VDA \leq 120^\circ$: Verified unconditionally.
- $\angle URQ \leq 120^\circ$: Solving the algebraic inequality corresponding to this angle condition yields exactly inequality I_2 .

3. Intersection Angle:

- We impose a stronger condition than required: we enforce that the angle between diagonals AQ and DR is $\leq 90^\circ$ (which implies $\leq 120^\circ$). This corresponds to the condition $\vec{AQ} \cdot \vec{DR} \geq 0$. Algebraic expansion confirms this is equivalent to inequality I_3 .

PART 2: ORTHOGONAL CONVEXITY CHECK

A set defined by the intersection of inequalities is orthogonally convex if, for each defining function $g_k(\mathbf{w}) \geq 0$ and each variable w_i , the function g_k is monotonic with respect to w_i (ensuring the cross-section is a connected interval). We verify this property for the system \mathcal{S} using symbolic differentiation.

Inequality I_1 : $g_1 = d(c + e - 1) + e(s + c)$.

- The function is linear in each variable individually. Linear functions are monotonic, satisfying the condition.

Inequality I_2 : $e \geq f(c, s, d)$, where f is the RHS.

- Variable e : Linear (monotonic).
- Variables c, s, d : We examine the partial derivatives of the bound f . Symbolic verification confirms:

$$\frac{\partial f}{\partial c} \leq 0, \quad \frac{\partial f}{\partial s} \leq 0, \quad \frac{\partial f}{\partial d} \geq 0.$$

Since the bound is monotonic in each parameter, the region defined by $e \geq f(c, s, d)$ is orthogonally convex.

Inequality I_3 : $g_3 = \text{LHS of } I_3$.

- Variables s, e : g_3 is linear in s and e (monotonic).
- Variable c : We compute $\frac{\partial g_3}{\partial c}$. Symbolic verification shows that $\frac{\partial g_3}{\partial c} \geq 0$ whenever $s + e \geq 1$. This condition is explicitly enforced by inequality I_4 .
- Variable d : We compute $\frac{\partial g_3}{\partial d}$. Symbolic verification shows that $\frac{\partial g_3}{\partial d} \leq 0$ whenever $c \leq 1 + d + s/2 + e/2$. This condition is explicitly enforced by inequality I_5 .

Inequalities I_4 and I_5 :

- These are linear inequalities, which inherently define orthogonally convex regions.

Conclusion: The region is the intersection of sets defined by functions that are monotonic in every coordinate axis (either unconditionally or conditioned on other inequalities in the set). Therefore, the intersection is orthogonally convex. \square

Step 9

Lemma 31 (Step 9). *If $e < s + 1$, then there exists a regular point E such that $|AE| \leq \max\{|AY|, |AZ|, |AR|, e + c - 1\}$.*

Proof. If R is a regular point, the statement is proved. We now assume R is a Steiner point. Let RN denote the next edge emanating from R in clockwise order. Let W be the intersection of the ray RN and the ray XA .

We proceed by case analysis.

Case 1: Point W lies on the line segment AX . Applying a technique identical to that used in the proof of Lemma 8, we can show that there exists a trapped regular point within the polygon $WXYZR$. Since $|AW| \leq |AX| < |AY|$, the distance from point A to this trapped point is bounded by:

$$\max\{|AY|, |AZ|, |AW|\}$$

Case 2: Point W does not lie on the line segment AX . In this case, a calculation yields $|AW| = e + c - 1 > 0$ and $|RW| = s + c$. Our objective is to prove the existence of a trapped regular point within the polygon $WXYZR$.

First, we prove by contradiction that N must lie on the line segment RW . Assume, for the sake of contradiction, that N does not lie on the segment RW . The condition $e < s + 1$ implies $|AW| < |RW|$. This would allow for a structural modification of the Steiner Minimal Tree (SMT)—by rerouting a path through AW instead of one corresponding to RW —that results in a shorter total length. This contradicts the minimality hypothesis of the SMT. Therefore, N must lie on the line segment RW .

Next, we analyze the properties of point N : If N is a regular point, our objective is met. If N is a Steiner point, let NT be the next edge emanating from N in clockwise order.

- If NT intersects AW , let M be the point of intersection. The condition $e < s + 1$ implies $|AM| < |NM|$. By a similar argument as before, a shorter tree could be constructed, which leads to a contradiction.
- If NT does not intersect AW , then should T also be a Steiner point, the extension of the subsequent clockwise edge from T must intersect either XY or YZ . By Lemma 16, it follows that a trapped regular point, let us call it E , exists within the polygon $WXYZR$.

In this final scenario, the distance $|AE|$ is bounded as follows:

$$|AE| \leq \max\{|AY|, |AZ|, |AR|, |AW|\}, \quad \text{where } |AW| = e + c - 1$$

This completes the proof. □

The preceding sections have established a complete theoretical framework for both verifying (via Theorem 6, Section B.4 and the previous subsection) and discovering (via Section B.2) new verification functions. This section presents the mathematical outcomes of applying this framework. The addition of these newly discovered and rigorously proven lemmas to our verification set is what ultimately enables the improvement of the lower bound on the Steiner ratio.

D. Algorithms and Implementation Details

D.1. Detail Algorithm for Reward Model

In this section, we present the detailed pseudocode and a comprehensive description of the core algorithm for our reward model. Given a set of verification functions \mathcal{F} , the algorithm will determine whether ρ can be obtained based on \mathcal{F} .

Feasibility Oracle

Algorithm 1 Feasibility Oracle

```

Input: Set of functions  $\mathcal{F} \subset \mathcal{F}_{\text{ver}}$ , parameter  $\rho$ .
Output: True if  $\rho$  is feasible based on verification functions  $\mathcal{F}$ , False otherwise
// Initialize with  $2^n$  regions covering the space
1 Initialization:  $Q \leftarrow \{\prod_{i=1}^n I_i \mid I_i \in \{[0, 1], [1, +\infty)\}\}$ 
2 while  $Q$  is not empty do
3   if iteration count exceeds threshold then
4     return False
5   Extract region  $B = \prod_{i=1}^n [l_i, r_i]$  with  $B \cap \text{Domain} \neq \emptyset$  from  $Q$ . Define  $I_\infty \leftarrow \{i \mid r_i = +\infty\}$  and
       $V \leftarrow \text{Vertices}(B)$ . Set  $\text{verified} \leftarrow \text{False}$ .
6   for  $F \in \mathcal{F}$  do
7     // Check monotonicity conditions
8     if  $F$  is monotonically decreasing in all  $i \in I_\infty$  then
9       if  $\max_{v \in V} F(v, \rho) \leq 0$  then
10       $\text{verified} \leftarrow \text{True}$ 
11    if not  $\text{verified}$  then
12       $k^* \leftarrow \arg \max_i (\text{if } i \in I_\infty$ 
         $\text{then } 1/l_i \text{ else } r_i - l_i)$ 
13       $m \leftarrow \text{if } k^* \in I_\infty \text{ then } 2 \cdot l_{k^*} \text{ else } (l_{k^*} + r_{k^*})/2$ 
14      Split  $B$  along dimension  $k^*$  at  $m$  into sub-regions  $B_{\text{left}}$  and  $B_{\text{right}}$ . Push  $B_{\text{left}}$  and  $B_{\text{right}}$  to  $Q$ 
15 return True

```

The algorithm recursively partitions \mathcal{W} into hyperrectangles, certifying that every region is covered by a verification function via the following steps:

1. **Initialization of Region Partitioning.** We maintain the queue Q of hyperrectangles that partition the search space. We initialize Q with the fundamental orthant splits to ensure the initial partition covers the entire unbounded space \mathcal{W} .
2. **Monotonicity Check for Unbounded Regions.** (Line 7) To handle regions extending to $+\infty$, we verify that the verification function f is monotonically non-increasing along the unbounded dimension. This ensures that the maximum value is attained at the finite lower bound. The implementation details of the monotonicity check are provided in Appendix Section B.4.
3. **Feasibility Verification for Bounded Regions.** (Line 8) For the finite vertices, we invoke the Vertex Maximum Property. By verifying $f(w) \leq 0$ at all vertices, we mathematically guarantee that the inequality holds for every point w within the region.
4. **Refinement via Subdivision.** (Lines 10-13) Unverified regions are subdivided along the dimension with the longest edge. For unbounded dimensions $[l, +\infty)$, we define a “logical length” of $1/l$ and apply a *geometric doubling strategy*, partitioning the interval into a bounded segment $[l, 2l]$ and a remaining unbounded tail $[2l, +\infty)$. This recursive process continues until the entire space is covered, leaving no unverified gaps.

D.2. Monotonicity Verification Algorithm

Monotonicity Check Procedure

Algorithm 2 Monotonicity Check Procedure

```

Input: Split  $\tau = (V^*, S^-, S^+, t^*)$ , Edge  $e$  with length parameter  $x$ 
Output: True if  $\frac{\partial F}{\partial x} \leq 0$  is guaranteed; False otherwise
    // 1. Contribution from removed structure  $S^-$  (Negative term)
1  $\delta_{S^-} \leftarrow \mathbb{I}(e \in S^-)$ 
    // 2. Contribution from connector  $t^*$  (Positive term)
2  $N_{t^*} \leftarrow \sum_{(u,v) \in t^*} \mathbb{I}(e \text{ lies on the path between } u \text{ and } v)$ 
    // 3. Contribution from the component  $S^+$  (Positive term)
3  $\delta_{S^+} \leftarrow 0$ 
4 for each pair of adjacent terminals  $(u, v)$  in  $S^+$  do
5   | if  $e$  lies on the path between  $u$  and  $v$  then
6     |   |  $\delta_{S^+} \leftarrow 1$ 
    |   // Verification Logic
7 if  $\delta_{S^-} + N_{t^*} + \delta_{S^+} = 0$  then
8   |   | return True; // Variable  $x$  is not involved in  $F$ 
9 if  $N_{t^*} + \delta_{S^+} \leq 1 \wedge \delta_{S^-} = 1$  then
10  |   | return True
11 else
12  |   | return False

```

Based on the lemmas above, we define the procedure to verify $\frac{\partial F}{\partial x} \leq 0$, which is presented in Algorithm 2.

D.3. Strategies for Handling Complex Splits

D.3.1. METHODS FOR HANDLING SPLITS WITH IMPLICIT REGULAR POINTS

When a split involves implicit regular points and utilizes edges connected to them (referred to as implicit edges), the validity condition and length functions for these edges are complex. Consequently, we only perform monotonicity checks for variables with respect to which the implicit edge lengths are constant. For these variables, the above procedure remains valid. For other variables, we do not regard the splitting function as having monotonicity with respect to these variables.

Specifically, under the settings in Sections E and C, we employ the following strategy:

- Splits involving the implicit points E : For variables s , c , and e , we do not assume monotonicity. For other variables, Algorithm 2 can be directly applied.
- Splits involving the implicit points F : For variables d , c , f (and u when D is Steiner), we do not assume monotonicity. For other variables, Algorithm 2 can be directly applied.

This conservative strategy is justified by the following observation: the verification bottlenecks (i.e., regions where the feasible ρ is minimized) typically occur near the origin of the parameter space \mathcal{W} . Therefore, complex splits only need to be applied to bounded regions, rather than unbounded ones. As a result, we adopt a conservative strategy regarding monotonicity for complex splits.

D.3.2. METHODS FOR HANDLING SPLITS WITH 4-POINT STEINER TREE

When a split comprises an S^+ that connects four terminals, the monotonicity of variable f can be verified using Algorithm 2, as established in Appendix B.4.2. For all other variables, monotonicity is not assumed.

This conservative strategy follows the same rationale as discussed above.

D.4. Enumeration of Valid Splits

To generate a rich candidate set of splitting functions, we perform an algorithmic enumeration of all topologically valid splits. The procedure is formally defined in Algorithm 3.

Definitions used in Algorithm:

- G : The graph representing the local Steiner substructure.
- V_{exp} : The set of explicit regular points (e.g., $\{A, B, D\}$ or $\{A, B, U, V\}$).
- W : The union of V_{exp} and the boundary connection points $\{Q, R\}$.
- V_{imp} : The set of available implicit regular points $\{E, F\}$.

Split Enumeration

Algorithm 3 Split Enumeration

Input: Graph G , Terminals V_{exp} , Boundary Set W , Implicit Points V_{imp}

Output: Final list of valid splits \mathcal{T}_{final}

// Phase 1: Pruning (Generate S^-)

```

1 Initialize  $\mathcal{T}_1 \leftarrow \emptyset$ 
2 for each non-empty subset  $V^* \subseteq V_{exp}$  do
3   for each subset of edges  $S^- \subseteq E(G)$  do
4     if all edges incident to  $V^*$  in  $G$  are included in  $S^-$  then
5       | Add  $(V^*, S^-)$  to  $\mathcal{T}_1$ 
// Phase 2: Re-optimization (Generate  $S^+$ )
6 Initialize  $\mathcal{T}_2 \leftarrow \emptyset$ 
7 for each tuple  $(V^*, S^-) \in \mathcal{T}_1$  do
8   Let  $G' = (V(G), E(G) \setminus S^-)$ 
9   Find connected components  $C_1, \dots, C_k$  of  $G'$  that contain at least one vertex from  $W \setminus V^*$ 
   // Enumerate all combinations of representatives
10  for each  $(p_1, \dots, p_k) \in V(C_1) \times \dots \times V(C_k)$  do
11    |  $S^+ \leftarrow \text{SMT}(\{p_1, \dots, p_k\})$ 
12    | Add  $(V^*, S^-, S^+)$  to  $\mathcal{T}_2$ 
// Phase 3: Re-connection (Generate  $t^*$ )
13 Initialize  $\mathcal{T}_{final} \leftarrow \emptyset$ 
14 Let  $V_{conn} = V_{exp} \cup V_{imp}$ 
15 for each tuple  $(V^*, S^-, S^+) \in \mathcal{T}_2$  do
16   for each subgraph  $t^*$  on vertices  $V_{conn}$  do
17     // Topology Check via Graph Contraction
18     Construct graph  $H$  from  $t^*$ : Contract all vertices in  $V_{conn} \setminus V^*$  into a single super-node  $\Omega$ 
19     if  $H$  is a spanning tree on the set  $V^* \cup \{\Omega\}$  then
20       | Add  $(V^*, S^-, S^+, t^*)$  to  $\mathcal{T}_{final}$ 
21 return  $\mathcal{T}_{final}$ 

```

E. Experimental Setup and Additional Results

E.1. Baseline Verification Functions

The construction of the baseline verification functions relies on a classical geometric result derived by [Du & Hwang \(1983\)](#). This result serves as a specific, manually proved instance of the “Trapped Regular Point” lemmas that our LLM agent aims to generalize.

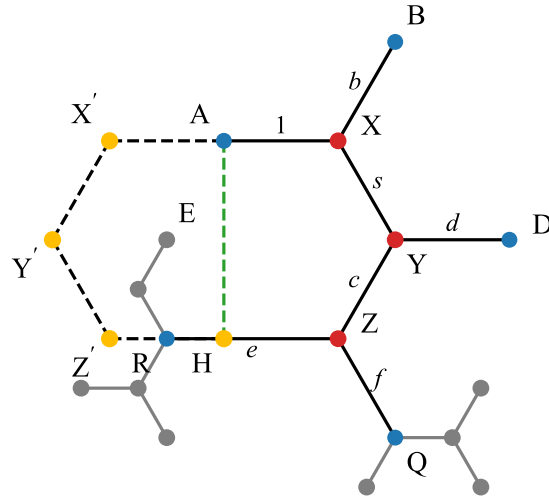


Figure 11. Sample of Subtree: D is regular

Recall the subtree of a Steiner Minimal Tree as shown in Figure 11. Let H be the orthogonal projection of A on the line ZR . Let the region $AX'Y'Z'H$ be the mirror reflection of the region $AXYZH$ with respect to AH .

Du & Hwang (1983) Lemma 2

Lemma 32 (Du & Hwang (1983) Lemma 2). If $c \leq 1$, there must exist a regular point E in the region $AXYZHZ'Y'X'$ that connects to A through Z .

Corollary 33. If $c \leq 1$, there must exist an implicit regular point E such that $|AE| \leq \max\{|AY|, |AZ|\}$.

Remark: It is important to note that the proof of Lemma 32 does not depend on the topological status of point A . Consequently, this trapping property applies universally to any such chain, regardless of whether the starting node is a regular point or a Steiner point. This allows us to apply the same logic symmetrically to the node D , even when D is a Steiner point connected to U and V .

Due to the symmetry of the Steiner structure, a similar rule applies to the chain starting at D .

Corollary 34. If $f \leq d$, there must exist an implicit regular point F such that its distance to the terminal is bounded. The bound depends on whether D is a regular point or a Steiner point:

- If D is a regular point, $|DF| \leq \max\{|DZ|, |DQ|\}$.
- If D is a Steiner point, $|UF| \leq \max\{|UY|, |UZ|, |UQ|\}$.

Based on the corollaries above, the baseline set $\mathcal{F}_{\text{ver}}^{(0)}$ comprises the verification functions resulted from all splits $\tau = (V^*, S^-, S^+, t^*)$ satisfying the following criteria:

1. The component S^+ satisfies $|S^+| \leq 3$.
2. The set of admissible edges in t^* is augmented to include the implicit connections (A, E) and (D, F) (or (U, F)). The length functions for these edges are conditional:

- Edge (A, E) :

$$L(A, E) = \begin{cases} \max\{|AY|, |AZ|\} & c \leq 1 \\ +\infty & c > 1 \end{cases}$$

- Edge (D, F) (when D is a regular point):

$$L(D, F) = \begin{cases} \max\{|DZ|, |DQ|\} & f \leq d \\ +\infty & f > d \end{cases}$$

- Edge (U, F) (when D is a Steiner point):

$$L(U, F) = \begin{cases} \max\{|UY|, |UZ|, |UQ|\} & f \leq d \\ +\infty & f > d \end{cases}$$

Impact on Monotonicity. When a split utilizes implicit edges (A, E) , (D, F) , or (U, F) , their length bounds depend on local geometric parameters. Establishing the required non-increasing property for these variables is non-trivial. Consequently, our system performs the monotonicity checks (as described in Appendix B.4) only for variables with respect to which the implicit edge lengths are constant.

Explanation of Steiner Ratio greater than 0.824 for Baseline Settings. Though we only cited technical lemmas from [Du & Hwang \(1983\)](#) as the baseline, and that work only claimed a proof for a Steiner ratio lower bound of $\rho = 0.8$, our initial ratio reached 0.8282, even surpassing the current SOTA of 0.824 by [Chung & Graham \(1985\)](#). This improvement is due to (1) prior work considered smaller topological structures. Our baseline setting directly considered topologies with a maximum chain length of 4, as shown in Figure 10, while previous human experts, constrained by computational capabilities, only considered topologies with a maximum chain length of 3. This allowed us to more accurately cover the parameter space, resulting in a higher lower bound; (2) prior work relied on manual proofs considering a relatively limited set of verification functions, whereas we leveraged computational mathematics to exhaustively enumerate all possible splits; (3) previous work employed looser scaling techniques, while we utilized more precise computational algorithms, eliminating gaps caused by arithmetic tricks.

E.2. Problem Decomposition and Search Space Reduction

During the iterative improvement phase, the LLM Agent focuses exclusively on refining the existence conditions for the implicit point E (associated with the chain starting at A). The conditions for the symmetric implicit point F (associated with the chain starting at D) remain fixed to the baseline criterion ($f \leq d$).

Consequently, the global verification problem is partitioned into four distinct sub-problems based on the topological status of D and the domain of the parameter f :

1. **Case 1:** D is a regular point, and $f \in [0, d]$ (F exists).
2. **Case 2:** D is a regular point, and $f \in (d, +\infty)$ (F does not exist).
3. **Case 3:** D is a Steiner point, and $f \in [0, d]$ (F exists).
4. **Case 4:** D is a Steiner point, and $f \in (d, +\infty)$ (F does not exist).

Reduction Strategy for Unbounded f . For Cases 2 and 4, where $f > d$, the implicit connection (D, F) (or (U, F)) is invalid and thus excluded from the connector graph t^* . In these scenarios, we apply a strict filtering policy: we only admit splits whose splitting functions are **monotonically non-increasing** with respect to f .

This monotonicity guarantees that the maximum value of the splitting function over the interval $(d, +\infty)$ is bounded by its value at $f = d$. Consequently, we mathematically substitute every occurrence of f with d in the verification functions. This operation effectively reduces the dimensionality of the parameter space \mathcal{W} by one. In these two cases, the variable f is removed entirely, and the verification proceeds on the projection of the hyperrectangles onto the remaining parameters.

Representative Regime for Evaluation. While our system rigorously verifies all four cases to establish the global lower bound, we restrict the detailed visualization and analysis in the main text to **Case 2** (D is Regular, $f \geq d$). This decision is justified by two empirical observations regarding the optimization landscape:

1. **Boundary Dominance:** The verification bottlenecks (regions where the feasible ρ is minimized) predominantly concentrate at the boundary $f = d$.
2. **Topological Degeneracy:** In cases where D is a Steiner point, the most critical constraints typically occur when the terminal edges ($|DU|$ and $|DV|$) approach zero length. In this limit, the structure topologically degenerates to the case where D is a regular point.

Consequently, Case 2 represents the most challenging and representative slice of the parameter space. Focusing on this regime allows us to demonstrate the system's efficacy on the “hardest” instances of the problem without redundancy.

F. LLM Agent and Prompts

F.1. Prompt for Searching Trapped Regular Point Lemmas

Prompt for Searching Trapped Regular Point Lemmas

PROMPT START

Role: You are an expert in Computational Geometry and Symbolic Logic.

Task: You need to derive a linear condition on three variables (a_2, a_3, a_4) that guarantees a polygonal chain is “trapped” within a bounded region, assuming the chain satisfies Minimum Steiner Tree properties.

Tools: You have access to a Mathematica execution environment.

You must follow the **6 Phases** below strictly.

PHASE 1: Geometric Definitions

Construct the coordinates of a polygonal chain A_0, A_1, \dots, A_n and a point D based on lengths a_i .

1. **Coordinate System:**
 - $A_0 = (0, 0)$
 - $A_1 = (1, 0)$ (Since $a_1 = 1$)
2. **Recursive Definition:** For $k \geq 2$, point A_k is derived from A_{k-1} by moving distance a_k at an inclination angle of $-60 \times (k - 1)$ degrees.
 - $A_2 = A_1 + a_2(\cos(-60^\circ), \sin(-60^\circ))$
 - $A_3 = A_2 + a_3(\cos(-120^\circ), \sin(-120^\circ))$
 - ... and so on.
3. **Point D:** D is connected to A_2 with length d at angle 0° .
 - $D = A_2 + (d, 0)$

PHASE 2: The Logical Implication Problem

You are working with two types of geometric properties.

1. **Properties (A) - Steiner Minimality:**
 - **Definition:** For any $0 \leq u < s \leq v \leq n$, the Euclidean distance satisfies $|A_u A_v| \geq a_s$.
 - **Meaning:** These are the constraints that the sequence a_i always satisfies.
2. **Properties (B) - The Polygon Trap:**
 - **Definition:** For $0 \leq u < s \leq v < n$, let H be the foot of the perpendicular from A_u to the line containing $A_v A_{v+1}$.
 - **The Trap:** IF H lies on the ray $A_v A_{v+1}$ AND the distance $|A_u H| < a_s$, THEN the entire tail of the chain (A_n) is trapped inside the polygon defined by vertices $A_u, A_{u+1}, \dots, A_v, H$.
 - **Meaning:** These are your goals. Proving one of these allows you to bound the distance to A_n .

CRITICAL INDEX CONSTRAINT:

For both property types $A(u, v)$ and $B(u, v)$, the index s (associated with the threshold length a_s) **MUST** satisfy the condition

$$u < s \leq v.$$

- *Example:* For a condition involving A_3 and A_4 (i.e., $u = 3, v = 4$), the **only** valid s is 4. You cannot use a_5 .

The Logical Goal:

Find a condition $C(a_2, a_3, a_4)$ such that:

$$\forall a_5, a_6, \dots (> 0) : [\text{Selected A-props are True}] \implies [\text{At least one Selected B-prop is True}].$$

PHASE 3: Condition Selection Strategy (Look-Up Only)

CRITICAL INSTRUCTION: Do NOT attempt to derive the algebraic expressions for conditions $A(u, v, s)$ or $B(u, v, s)$ yourself. Use the exact algebraic forms provided in the list below.

1. **Analyze the Box:** Check the provided Box values against the B conditions in the list. Identify which ones are likely to hold (i.e., where the inequality is satisfied or close to satisfied).
2. **Select Constraints:** Select a small subset (e.g., 1 B property and 0–3 A properties) that seem most relevant to the Box.
3. **Formulate Logic:** You want to prove that the A constraints prevent a_5, a_6 from violating the B goal. It is OK that B goals do not involve a_5, a_6 , in which case you may not need A properties.

IMPORTANT Tip: You should first check B properties with $v \leq 4$ and identify if there are any that already hold. In these cases, you do not need to derive upper bound for a_5 .

Tips: In order to pose upper bound on a_5 , you can typically use $A(0, 5, 5)$.

Variable Instantiation (WARNING):

- The conditions in the list below contain the variable a_s . When you select a condition $A(u, v)$ or $B(u, v)$, you must replace a_s with a specific a_k .
- **CONSTRAINT:** You must ensure $u < k \leq v$.
- **ERROR TRAP: Do NOT** use $B(3, 4)$ with a_5 . Since $u = 3, v = 4$, the condition $s \leq v$ requires $s \leq 4$. Using $s = 5$ is geometrically invalid.

The Provided List (Algebraic Forms):

```

Example: A(u, v, s) represents the (A) condition for points |A_u A_v| >= a_s
A(0, 1): 1 >= a_s
A(0, 2): 1 + a2 + a2^2 >= a_s^2
A(0, 3): 1 + a2 + a2^2 - a3 + a2*a3 + a3^2 >= a_s^2
A(0, 4): a2^2 + a3^2 + a2*(1 + a3 - a4) + a3*(-1 + a4) + (-1 + a4)^2 >= a_s^2
A(0, 5): 1 + a2^2 + a3^2 - 2*a4 + a4^2 + a2*(1 + a3 - a4 - 2*a5) + a3*(-1 + a4 - a5) - a5 + a4*a5 + a5^2 >= a_s^2
A(0, 6): 1 + a2^2 + a3^2 - 2*a4 + a4^2 - a5 + a4*a5 + a5^2 + a3*(-1 + a4 - a5 - 2*a6) + a2*(1 + a3 - a4 - 2*a5 - a6) + a6 - a4*a6 + a5*a6 + a6^2 >= a_s^2
A(1, 2): a2 >= a_s
A(1, 3): a2^2 + a2*a3 + a3^2 >= a_s^2
A(1, 4): a2^2 + a3^2 + a2*(a3 - a4) + a3*a4 + a4^2 >= a_s^2
A(1, 5): a2^2 + a3^2 + a4^2 + a2*(a3 - a4 - 2*a5) + a3*(a4 - a5) + a4*a5 + a5^2 >= a_s^2
A(1, 6): a2^2 + a3^2 + a4^2 + a4*a5 + a5^2 + a3*(a4 - a5 - 2*a6) + a2*(a3 - a4 - 2*a5 - a6) - a4*a6 + a5*a6 + a6^2 >= a_s^2
A(2, 3): a3 >= a_s
A(2, 4): a3^2 + a3*a4 + a4^2 >= a_s^2
A(2, 5): a3^2 + a4^2 + a3*(a4 - a5) + a4*a5 + a5^2 >= a_s^2
A(2, 6): a3^2 + a4^2 + a5^2 + a3*(a4 - a5 - 2*a6) + a4*(a5 - a6) + a5*a6 + a6^2 >= a_s^2
A(3, 4): a4 >= a_s
A(3, 5): a4^2 + a4*a5 + a5^2 >= a_s^2
A(3, 6): a4^2 + a5^2 + a4*(a5 - a6) + a5*a6 + a6^2 >= a_s^2
A(4, 5): a5 >= a_s
A(4, 6): a5^2 + a5*a6 + a6^2 >= a_s^2
A(5, 6): a6 >= a_s

```

```

B(0, 1): False
B(0, 2): (1 - a2)/2 >= 0 && ((Sqrt[3]*(1 + a2))/2 <= a_s)
B(0, 3): (2 + a2 - a3)/2 >= 0 && ((Sqrt[3]*(a2 + a3))/2 <= a_s)
B(0, 4): (1 + 2*a2 + a3 - a4)/2 >= 0 && ((Sqrt[3]*(-1 + a3 + a4))/2 <= a_s)
B(0, 5): (-1 + a2 + 2*a3 + a4 - a5)/2 >= 0 && ((Sqrt[3]*(-1 - a2 + a4 + a5))/2
<= a_s)
B(1, 2): False
B(1, 3): (a2 - a3)/2 >= 0 && ((Sqrt[3]*(a2 + a3))/2 <= a_s)
B(1, 4): (2*a2 + a3 - a4)/2 >= 0 && ((Sqrt[3]*(a3 + a4))/2 <= a_s)
B(1, 5): (a2 + 2*a3 + a4 - a5)/2 >= 0 && ((Sqrt[3]*(-a2 + a4 + a5))/2 <= a_s)
B(2, 3): False
B(2, 4): (a3 - a4)/2 >= 0 && ((Sqrt[3]*(a3 + a4))/2 <= a_s)
B(2, 5): (2*a3 + a4 - a5)/2 >= 0 && ((Sqrt[3]*(a4 + a5))/2 <= a_s)
B(3, 4): False
B(3, 5): (a4 - a5)/2 >= 0 && ((Sqrt[3]*(a4 + a5))/2 <= a_s)
B(4, 5): False

```

The Required Box:

Your condition must cover this region:
 {Bottleneck}

PHASE 4: Mathematica Derivation

Use the tool to solve the implication.

Step 4.1: Attempt Derivation

Run the following logic in Mathematica using the expressions copied from the list:

```

(* Define the logic: ForAll tail_vars, (Steiner_Constraints) implies (Trap_Goal)
 *)
Reduce[
  ForAll[{a5, a6},
    a5 > 0 && a6 > 0 && <Selected_A_Props>,
    <Selected_B_Props>
  ] && a2 > 0 && a3 > 0 && a4 > 0,
  {a2, a3, a4}
]

```

Tip: If the result is non-linear, relax it to a linear inequality that still covers the Box.

Step 4.2: Verification

Verify your derived condition <Cond>:

```

Reduce[
  !ForAll[{a5, a6}, a5>0 && a6>0 && <Selected_A_Props>, <Selected_B_Props>
  && a2 > 0 && a3 > 0 && a4 > 0
  && <Cond>,
  {a2, a3, a4}
]

```

The output **MUST** be False.

Important: You MUST verify the implication in the **ENTIRE** domain, not in the Test Box.

PHASE 5: Upper Bound Calculation

If the logic in Phase 4 holds, the point A_n is trapped in the polygon $A_u \dots A_v H A_u$ defined by your selected B property. You must now calculate the specific coordinates of these vertices to determine the maximum distance.

1. Identify and Fix Vertices ($A_u \dots A_v$):

- **Case $v < 5$:** The points A_1, \dots, A_4 are fully determined by the input parameters a_2, a_3, a_4 . Use their standard coordinates.
- **Case $v = 5$:** The point A_5 depends on the variable a_5 . To fix this:

- In Phase 4, you should have ensured the condition implies a bound on a_5 . Specifically, you may **ADD another goal** to your derivation: $a_5 \leq a_2 + a_3$.
- For the Upper Bound calculation here, assume the “worst case” where a_5 reaches this limit: set $a_5 = a_2 + a_3$.
- Calculate the coordinates of A_5 using this substituted value.

2. Calculate Vertex H:

- H is the foot of the perpendicular from A_u to the line defined by A_v and direction $-60v^\circ$.
- Since A_u and A_v are now fixed (based on steps above), explicitly calculate the (x, y) coordinates of H .

3. Affine Constraint (CRITICAL):

- You **MUST** ensure that the coordinates (x, y) of **every** vertex in the trap polygon (A_u, \dots, A_v, H) are expressed as **Affine Functions** of a_2, a_3, a_4 .
- *Format:* $x = C_0 + C_1a_2 + C_2a_3 + C_3a_4$.
- This ensures the upper bound function remains simple and robust.

4. Compute Upper Bounds:

- $\text{MaxDist}_A = \max(|A_0P|)$ for all $P \in \{A_u, \dots, A_v, H\}$.
- $\text{MaxDist}_D = \max(|DP|)$ for all $P \in \{A_u, \dots, A_v, H\}$.

PHASE 6: Implementation & Output Requirements

Detailed Derivation: Show how you choose the A / B properties and how you derived the final condition.

Upper Bound: If A_5 is involved in the trapping polygon, **EXPLICITLY** state the upper bound of a_5 .

Mathematica Output: Paste the code and the output confirming the `False` result for the implication checks.

Constraints:

1. **Linearity:** The final condition on a_2, a_3, a_4 must be linear.
2. **Generality:** Do not hardcode the box values. The condition must be algebraic.
3. **Safety:** You DO NOT need to include inequalities like $a_2 > 0$ at 0.

Final Output: Provide a C++ code block containing these exact functions:

```
// Returns true if a2, a3, a4 satisfy the derived linear condition.
bool X_cond(double a2, double a3, double a4) {
    // Your linear inequality here
}

// Returns the upper bound of dist(A0, An) based on the trap polygon vertices.
double AX_upper_bound(double a2, double a3, double a4) {
    // Return max distance to polygon vertices
}

// Returns the upper bound of dist(D, An).
double DX_upper_bound(double a2, double a3, double a4, double d) {
    // Return max distance from D to polygon vertices
}
```

If you fail to find a valid condition after rigorous attempts, return `false` and 0.0.

CRITICAL WARNING: Do NOT attempt to do anything that violates the above rules. Feel free if you indeed fail to find a valid condition.

— END OF PROMPT —

F.2. Prompt for Searching Valid 4-Point Steiner Tree Lemmas

Prompt for Searching Valid 4-Point Steiner Tree Lemmas

PROMPT START

Role: You are an expert Computational Geometer and Mathematician.

Objective: Derive a simplified, robust condition $P(b, c, d, s, e)$ that guarantees the existence of a specific Steiner Tree.

Constraint: The condition you find must be "Axis-Parallel Segment Closed" (APSC).

Tools: You have access to a Mathematica execution environment and a Python execution environment.

PHASE 1: Geometric Definitions

Construct the following points in the 2D plane based on these vector instructions.

- **A:** $(0, 0)$
- **X:** From A, move length 1 at angle 0° .
- **Y:** From X, move length s at angle -60° .
- **B:** From X, move length b at angle 60° .
- **D:** From Y, move length d at angle 0° .
- **P:** From Y, move length c at angle -120° .
- **Q:** From P, move length d at angle -60° .
- **R:** From P, move length e at angle 180° .

The domain of the variables is $b \geq 0 \ \&\& c \geq 0 \ \&\& d \geq 0 \ \&\& s \geq 0 \ \&\& e \geq 0$.

Note: Although Points X, Y, P are used for construction, your final task focuses on the Steiner Tree for points {A}, {B}, {C}, {D}.

PHASE 2: The Existence Logic (Type {A}{B}-{C}{D})

You are investigating the existence of an $(\{A\}\{B\})-(\{C\}\{D\})$ type Steiner Tree. For this specific type, define the auxiliary points U and V as follows:

1. **Point U:** Rotate point $\{B\}$ 60° counter-clockwise around $\{A\}$.
2. **Point V:** Rotate point $\{D\}$ 60° counter-clockwise around $\{C\}$.

The Exact Existence Conditions (E_{exact}) are:

1. **Convexity:** The quadrilateral formed by $\{A, B, C, D\}$ must be convex.
2. **Internal Angles:** The angles $\angle UCD$, $\angle UDC$, $\angle VAB$, and $\angle VBA$ must all be $\leq 120^\circ$.
3. **Crossing Angle:** Let θ be the angle between diagonal vectors \vec{AC} and \vec{BD} . The condition is $\theta \leq 120^\circ$.
 - *Relaxation Hint:* You may relax this third condition to $\theta \leq 90^\circ$ (which is $\vec{AC} \cdot \vec{BD} \geq 0$) if it helps simplify the math.

The condition for "convex quadrilateral" can be formulated as follows: For any three adjacent points x, y, z (in clockwise order), the cross product of vectors xy and yz is less than or equal to zero.

The condition that the angle between vectors u and v is less than or equal to 120 degrees can be expressed using the cosine rule or the dot product of vectors, namely: vectors u and v form an angle $\leq 120^\circ$ iff

$$2 \operatorname{dot}(u, v) + (|u| |v|) \geq 0.$$

You may relax it to $\operatorname{dot}(u, v) \geq 0$ if possible.

PHASE 3: Deriving the Relaxed Condition P

The exact conditions above are too complex. You must find a **sufficient condition** $P(b, c, d, s, e)$ such that $P \implies E_{exact}$.

Requirements for Condition P (APSC Property):

Definition: A condition P satisfies APSC if, for any line parallel to one of the coordinate axes, the set of points within the domain (variables ≥ 0) that satisfy the condition forms a single connected interval.

To satisfy APSC, P must be the conjunction of inequalities from the following allowed categories only:

1. **Linear or Multilinear:** Inequalities that are linear in each variable separately.
2. **Quadratic:** Inequalities in the form $Ax^2 + Bx + C \geq 0$ (or ≤ 0), subject to monotonicity rules explained in the prompt.
3. **Functional Boundaries:** Inequalities in the form $e > f(b, c, s, d)$ or $e < f(b, c, s, d)$, where monotonicity of f must be verified.

Coverage Requirement:

Your condition P must be general (not hardcoded numbers), but it must strictly cover the following "Test Box": {Bottleneck}

Important: You MUST verify the APSC Property in the **ENTIRE** domain, not in the Test Box.

PHASE 4: Verification Protocol

You must verify your work using Mathematica logic.

Step A: Write Mathematica code to compute the exact expressions for the 6 existence inequalities (Convexity + Angles).

Step B: Define your relaxed condition `condP`.

Step C: Verify Implication. You must run a command equivalent to this logic (check each inequality separately):

```
Reduce[ !<ExactCondition_i> && condP && b>=0 && c>=0 && d>=0 && s>=0 && e>=0, {vars} ]
```

If this returns `False`, your condition is valid. If it returns `True` or an expression, your condition is invalid.

Tips: Reformulate $2 \dot{u} \cdot v + (|u| |v|) \geq 0$ into $\dot{u} \cdot v \geq 0 \parallel 4 \dot{u} \cdot v \leq |u|^2 |v|^2$ for faster speed when verifying.

Constraint: Do not put all checks in one `Reduce` call. It will time out. Check each inequality individually against P .

Important: You MUST verify the implication in the **ENTIRE** domain, not in the Test Box.

PHASE 5: Output Requirements

1. **Detailed Derivation:** Show how you calculated coordinates and how you derived the relaxed inequalities.
2. **APSC Proof:** Provide a logical argument explaining why your condition P satisfies the APSC property, specifically addressing the Linearity/Monotonicity requirements for each part of your condition.
3. **Mathematica Output:** Paste the code and the output confirming the `False` result for the implication checks.
4. **C++ Implementation:**

Provide a C++ code block containing these exact functions:

```
// Returns true if your condition $P$ is met.
bool steiner_cond(double b, double c, double d, double s, double e) {
    // Your condition here
}

// Returns the total length of the ({A}{B}-{C}{D}) type Steiner tree, which is
// exactly |UV|, the distance between U and V.
```

```
double steiner_length(double b, double c, double d, double s, double e) {  
    // Return the distance between U and V  
}
```

Important: Do NOT use the Test Box values inside the C++ code. The code must be a general algebraic formula.

If you fail to find a valid condition after rigorous attempts, return **false** and 0.0.

— END OF PROMPT —